ADVANCED MATERIALS INTERFACES

Surface Patterning of Hydrogel Biomaterials to Probe and Direct Cell–Matrix Interactions

Brizzia G. Munoz-Robles, Irina Kopyeva, and Cole A. DeForest

Due to their mechanical and structural similarity to native tissues, hydrogel biomaterials have gained tremendous popularity for applications in 3D tissue culture, therapeutic screening, disease modeling, and regenerative medicine. Recent advances in pre- and post-synthetic processing have afforded anisotropic manipulation of the biochemical, mechanical, and topographical properties of biocompatible gels, increasingly in a dynamic and heterogeneous fashion that mimics natural processes in vivo. Herein, the current state of hydrogel surface patterning to investigate cellular interactions with the surrounding matrix is reviewed, both in techniques utilized and biological findings explored, and the perspective on proposed future directions for the field is offered.

1. Hydrogel Biomaterials as Extracellular Matrix Mimetics

The extracellular matrix (ECM) is the noncellular component present in all tissues with important structural and biological roles. It acts as physical scaffolding for cells, offers adhesion sites, and initiates crucial biochemical and biophysical cues required for tissue differentiation, morphogenesis, and homeostasis (**Figure 1**). The ECM composition varies

B. G. Munoz-Robles, I. Kopyeva, Prof. C. A. DeForest
Department of Bioengineering
University of Washington
3720 15th Ave NE, Seattle, WA 98105, USA
E-mail: ProfCole@uw.edu
Prof. C. A. DeForest
Department of Chemical Engineering
University of Washington
3781 Okanogan Lane NE, Seattle, WA 98195, USA
Prof. C. A. DeForest
Department of Chemistry
University of Washington
4000 15th Ave NE, Seattle, WA 98195, USA
Prof. C. A. DeForest
Institute for Stem Cell & Regenerative Medicine
University of Washington
850 Republican Street, Seattle, WA 98109, USA
Prof. C. A. DeForest
Molecular Engineering & Sciences Institute
University of Washington
3946 W Stevens Way NE, Seattle, WA 98195, USA

The ORCID identification number(s) for the author(s) of this article can be found under https://doi.org/10.1002/admi.202001198.

from tissue to tissue, but is generally composed of proteins such as collagen, laminin, elastin, and fibronectin; glycosoaminoglycans (GAGs) such as heparin, chondroitin sulfate, and keratan sulfate; and polysaccharides such as hyaluronic acid (HA). All of these ECM components can directly interact with cells through specific cellular receptors or bind growth factors that are released upon ECM remodeling. For instance, the Arg–Gly–Asp (RGD) peptide motif found within fibronectin, collagen, and other ECM molecules, has long been known to mediate cell adhesion through integrin signaling.[1] Moreover, the composition of the ECM affects microscopic and bulk tissue mechanics and topography.[2]

These cues themselves are dynamic, with matrix composition, mechanics, and architecture changing during development, aging, and disease processes.[3] Where and when these cues are turned on is critical in both normal homeostatic tissue maintenance and disease progression. During development, biochemical gradients are especially critical, and it has been shown that developing cells exhibit a concentration-dependent response to morphogen gradients of bone morphogenetic protein (BMP), sonic hedgehog (Shh), transforming growth factor-β (TGF-β), and fibroblast growth factors.[4] As another example, epicardial stiffness increases approximately threefold during development, while myocardium postinfarction forms a fibrotic scar that is three to four times stiffer than the surrounding tissue.[5] Tumor tissue also displays a gradient of matrix elasticity.[6] Additionally, growth factor gradients and surface roughness differences are known to guide fibroblast migration during wound healing.[7]

Since the large number of uncontrollable variables makes it challenging to probe the effects of dynamic and heterogeneous cues found in vivo, researchers have turned to synthetic platforms with customizable properties to elucidate their individual contributions. Hydrogels, water-swollen polymer-based networks that can be made from either natural or synthetic precursors, offer an ideal model matrix.[8,9] The wide range of materials and chemistries employed affords tight control over many biochemical and biophysical properties, such as ligand presentation, matrix mechanics, and surface topography.[10] Several complementary techniques have also been introduced to further modify hydrogel properties in space and time. This review will highlight recent strategies for making patterned hydrogel surfaces and opportunities in using them to probe and direct cell fate.
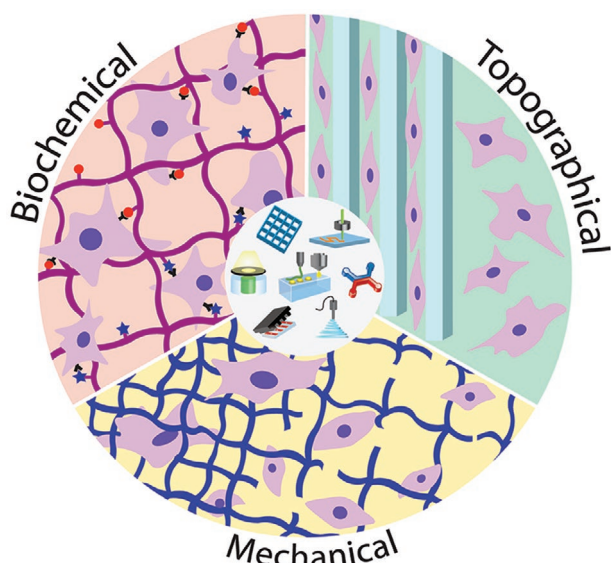
Figure 1. The ECM influences cellular function through spatiotemporally presented biochemical, topographical, and mechanical cues. Several recurring and core processing techniques have been used to pattern these signals within hydrogel biomaterials.

2. Materials and Methods to Pattern Hydrogel Substrates

2.1. Hydrogel Materials and Fabrication

Hydrogel networks can be fabricated from a variety of monomers, both natural and synthetic in origin. Common naturally derived materials include collagen and its hydrolyzed form, gelatin; alginate; HA; fibrin; and decellularized ECM. Common synthetic hydrogel precursors include polyacrylamide (PA), poly(ethylene glycol) (PEG) and its functionalized derivatives, as well as more complex copolymers such as pluronics, which consist of two hydrophilic poly(ethylene oxide) blocks flanking a hydrophobic poly(propylene) structure. The mechanism of hydrogel network assembly is different across systems; for instance, collagen undergoes a sol–gel transition at 37 °C, alginate forms a gel when monovalent cations are replaced with divalent cations (e.g., Ca^{2+}), and fibrin requires the addition of thrombin to catalyze the polymerization reaction. Others such as HA, gelatin, and PEG can be modified with groups such as acrylates, methacrylates, and styrenes, which crosslink into stable gels via free radical polymerization. PA gels are also formed by a vinyl addition reaction initiated by a free radical-generating system. Additionally, click reactions—highly specific and controllable bioorthogonal chemistries characterized by a high thermodynamic driving force—including thiol-ene, azide-alkyne cycloaddition, and oxime ligation are increasingly utilized for hydrogel formation.

2.2. Common Techniques for Gel Patterning

Many techniques exist to modify the chemical, mechanical, and topographical properties of hydrogel surfaces so as to recreate native ECM characteristics in vitro. Chemical surface patterning is used for the introduction of biologically relevant cues in a spatiotemporally controlled manner on or within hydrogels. Biophysical patterning has also become an important area of research, encompassing topographical structures on hydrogels that mimic those present in the ECM (e.g., pores, fibers, ridges), as well as changes in local stiffness and viscoelasticity.[2,11] User-controlled size, shape, and periodicity of hydrogel structures has been primarily achieved through photolithography, soft lithography, microfluidic patterning, controlled mixing, inkjet printing, and electron-beam (e-beam) lithography (**Figure 2**). In this section, we compare and contrast some of these common techniques for hydrogel patterning.

2.2.1. Photolithography

Mask-based photolithography, first popularized in the semiconductor industry, is a patterning process in which an optical mask is used to selectively constrain light exposure onto a photosensitive layer, confining photochemical reactions to illuminated regions. Patterning resolution is defined by the wavelength of light utilized, scattering of the underlying material, and the fidelity of the utilized photomask. Though comparatively expensive photomasks (e.g., chrome printed on glass) are required for sub-micrometer patterning control, lower resolution masks (e.g., black ink printed on transparency film) can be generated rapidly at low cost. Mask-based photolithography is a diffraction-limited process—one that ultimately affords patterning control only in the x–y dimensions.

To address this challenge, light-based patterning can be achieved by laser-scanning lithography (LSL). LSL is a maskless approach that can be used to create patterned features with high resolution. In LSL, a focused laser beam is raster- or serially scanned over a surface with varying intensities to create patterns in the photoresist. Though laser-scanning hardware is comparatively expensive to that utilized in mask-based photolithography, computer-controlled scanning enables complex patterns to be generated on the fly at no cost beyond the instrument. LSL for the fabrication and patterning of hydrogels can be performed by either single-photon (SP-LSL) or multiphoton lithography (MP-LSL). Both allow for sub-micrometer-level control over feature size in x–y; MP-LSL additionally permits single-micrometer resolution in the z dimension.

In addition to providing micrometer-scale patterning resolution over where hydrogel modification occurs, photolithographic material alteration can also be specified in time, enabling for dynamic modulation of gel surfaces in the presence of live cells. Furthermore, light-based techniques can proceed in a contactless manner using cytocompatible chemistries, which can be readily performed about and within living samples without fear of contamination or cellular damage.[12]

2.2.2. Electron-Beam Lithography

E-beam patterning is another maskless technique that can be used for patterning hydrogel surfaces with exceptionally high resolution on the nanoscale level.[13] In its most conventional
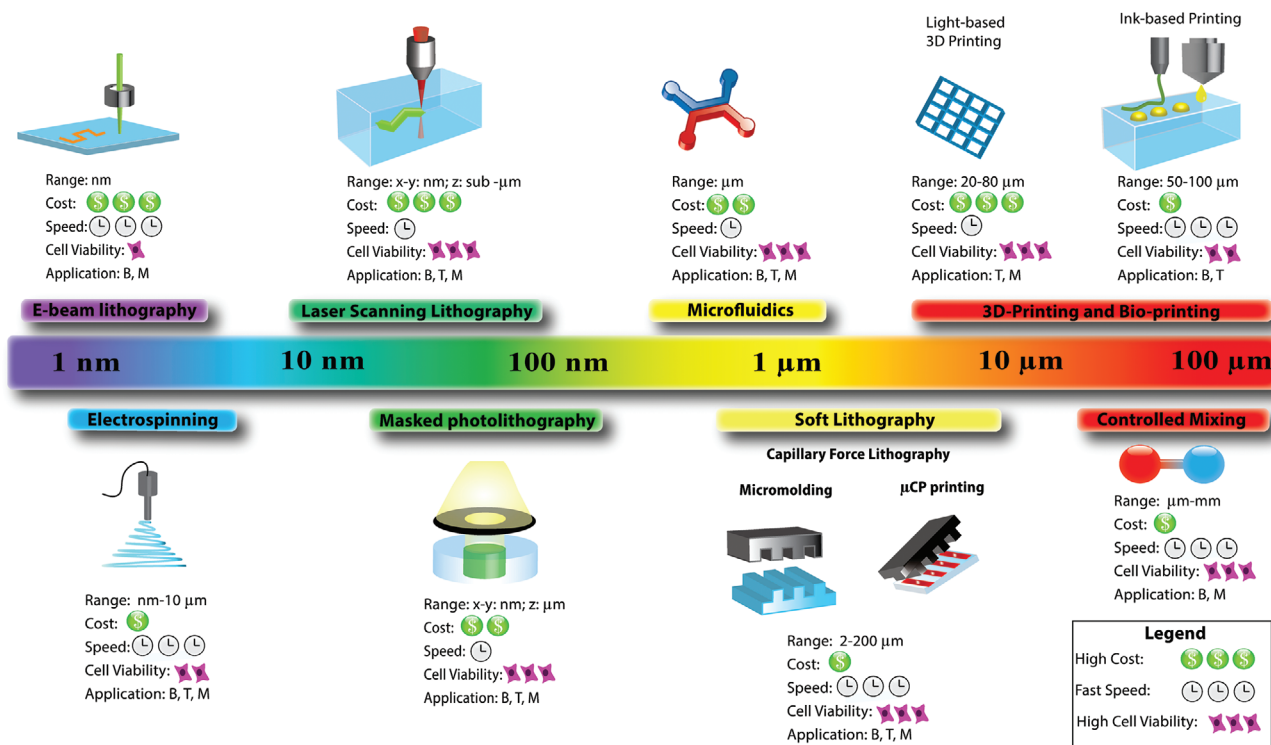
Figure 2. Several common techniques are used for biochemical (B), topographical (T), and mechanical (M) surface patterning of hydrogels over a wide range of length scales. Each offers different advantages with respect to resolution, cost, speed, and cytocompatibility.

form, a polymer film is coated on a Si substrate and subsequently exposed to a focused e-beam. The directed electrons crosslink (positive resist) or degrade (negative resist) the polymer. Limitations of e-beam lithography include its high equipment cost and slower speed. Though e-beam patterning affords structures with much higher resolution than those that are photolithographically generated, the requirement to perform e-beam modification under vacuum precludes its usage in the presence of living cells.

2.2.3. Soft Lithography

Soft lithography, first introduced by the Whitesides group, has emerged as a more cost-effective competitor to photo- and e-beam lithography while offering similar resolution. It encompasses a range of microfabrication techniques utilizing elastomeric substrates to transfer patterns by molding or stamping biochemicals.[14] Rather than fabricating the pattern anew each time, this technique enables rapid prototyping by replicating a master mold. In the first step, a master mold is created by photolithographical etching of a thin film of photoresist atop a silicon wafer.[15,16] Typically, an elastomer is then cast as a negative replica of the Si master; polydimethylsiloxane (PDMS) is most commonly employed, though other polymers can be used to make a replica mold. PDMS is generally favored due to its beneficial properties: it is deformable enough to achieve conformal contact on surfaces with micrometer and nanometer resolutions; its elastic nature allows for easy release; it is

optically transparent, enabling curing of prepolymers being molded; and finally, it is durable, enabling multiple molding events with no noticeable degradation.[15] The main disadvantages of soft lithography are the potential for distortion of patterns of the mold or stamp due to deformation of the elastomer, limitations in patternable geometries, and a somewhat limited range of materials that can be patterned.

While multiple soft lithographical techniques exist, only a few are commonly used for hydrogel patterning. Here, soft lithography will encompass micromolding, microcontact printing (μCP), and micromolding in capillaries. Micromolding duplicates information (e.g., ridges, grooves, microposts, pits) from the original Si mold by generating a negative of the PDMS mold. This procedure allows for one-step reproduction of complex topographical features, whereas photolithography cannot mass produce such structures.[15] Microcontact printing, a subdivision of soft lithography typically utilized in biochemical patterning, enables modification of surfaces by direct transfer of an "ink" with a stamp in contact with the polymeric solution.[14] Stamps with patterned features are placed in direct contact with the hydrogel, and immobilized biomolecules on the stamp are transferred by physical adsorption only in areas where the stamp is in close contact with the surface.[17] Lastly, capillary force lithography (CFL), popularized by the Suh group, has seen a rise in usage for topographical patterning. A patterned PDMS mold is placed on a polymer surface, which is heated past the glass-transition temperature; capillary action forces the polymer melt into the void space of the mold, thereby generating a negative replica of the mold.[18]
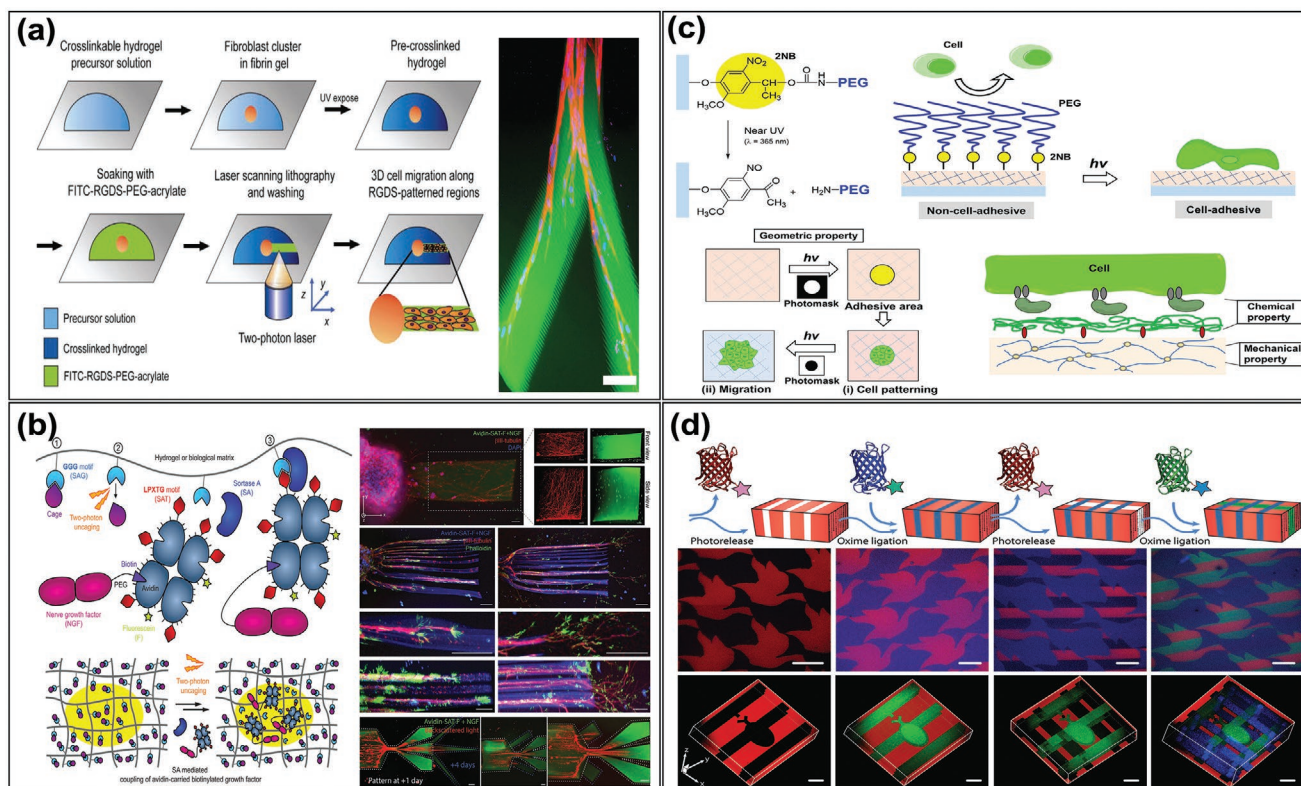
**ADVANCED
SCIENCE NEWS**

www.advancedsciencenews.com

**ADVANCED
MATERIALS
INTERFACES**

www.advmatinterfaces.de

Figure 3. Photolithographic patterning of biochemical cues. a) Left: 3D RGDS patterning by MP-LSL. Right: Fibroblasts undergoing 3D migration within RGDS-patterned regions inside enzyme-sensitive PEG hydrogels. Scale bar = 100 µm. Reproduced with permission.[77] Copyright 2008, Elsevier Ltd. b) Left: Schematic for MP-LSL patterning based on photo-uncaging and an orthogonal enzymatic coupling that enables immobilization of avidin-linked biotinylated growth factors. Right: Patterns of NGF in HA gels guide axonal growth from sensory neurons in 3D. Reproduced with permission.[91] Copyright 2020, Wiley-VCH. c) Design and principle of photoactivatable surface patterning using *o*NB photocleavage to control cell adhesion. Reproduced with permission.[58] Copyright 2018, American Chemical Society. d) Mask-based and MP-LSL photolithographic techniques used to reversibly immobilize proteins within PEG hydrogels. Scale bar = 100 µm. Reproduced with permission.[54] Copyright 2019, Nature Publishing Group.

2.2.4. Inkjet Printing

In its most conventional form, inkjet printing of biomolecules on hydrogel surfaces is accomplished by dispensing small volumes of a bioink onto a hydrogel surface. Biomolecules can be dropped on demand or continuously.[19] Inkjet printing has a spatial resolution of 50–300 µm and the amount of transferred material can be controlled by the printed spot size and the solute concentration in the ink.[20] Advantages of inkjet printing are its high printing speed and relatively low cost. However, the viscosity of the bioink is a limiting factor, and the excessive stress can damage cell functionality and viability.[21] Furthermore, the patterned resolution and feature size of inkjet printing lags considerably beyond alternative techniques including microcontact printing.[22,23]

3. Biochemical Patterning of Hydrogel Substrates

The native ECM is a highly dynamic and heterogeneous microenvironment that regulates the presentation of biochemical signals, including small molecules, peptides, and proteins. The spatial orientation and the timed presentation of these cues affect how they are translated into signals that guide cell fate.

Therefore, to recapitulate the ECM's dynamic nature, efforts have focused on developing in vitro culture platforms that enable spatial and temporal control over biochemical presentation on and within hydrogels. This section describes techniques available to pattern bioactive molecules on hydrogel surfaces and their use to control and study cell adhesion, spreading, movement, and differentiation.

3.1. Photolithography

Photolithography is the most common and versatile tool for controlling the spatial and temporal presentation of biochemical cues in hydrogels (**Figure 3**). Mask-based and laser-scanning lithographic strategies can be employed to immobilize and/or remove biomolecules (e.g., small molecules, peptides, proteins) from biomaterial surfaces.[24–29] In "additive patterning," light is used to drive photochemical reactions to functionalize hydrogel surfaces directly. In contrast, "subtractive patterning" occurs when light is used to remove biomolecules from gel surfaces, most commonly through a photoscission reaction. Finally, "reversible patterning" utilizes sequential light exposures, potentially with different wavelengths, to first immobilize and subsequently release species from gel surfaces.

3.1.1. Mask-Based Photolithography

Additive Patterning: Spatially controlled immobilization of biochemical cues utilizing mask-based lithography was first demonstrated by the West group in 2006, where acrylate–PEG–Arg–Gly–Asp (RGD) peptides were selectively photopolymerized into user-defined regions within a PEG–diacrylate (PEGDA) hydrogel.[30] This technique was later used to show concentration- and width-dependent angiogenesis of endothelial cells seeded on adhesion peptide Arg–Gly–Asp–Ser (RGDS)-patterned PEGDA hydrogels.[31] While these studies introduced an exciting new area with tremendous potential, using PEGDA for postgelation patterning is not without drawbacks: 1) it is difficult to accurately control the free groups available after initial crosslinking and polymerization for further functionalization, 2) there is an interdependence between the number of groups available for functionalization and the mechanical properties of the hydrogel, and 3) the chain-growth nature of polymerization hinders molecular control over peptide density within the gel. To overcome these limitations, patterning approaches exploiting molecular photocages have been incorporated to control biochemical cue activity. In one example, Lee et al. engineered a 3-(4,5-dimethoxy-2-nitrophenyl)-2-butyl ester (DMNPB) protecting group on an RGD peptide, rendering it inactive.[32] Upon light exposure, the photocage was removed and the peptide activated. The photocaged RGD was acrylated and subsequently incorporated into PEGDA hydrogels. Spatial activation of the caged bioligand was achieved by exposing the hydrogel to ultraviolet (UV) light through a mask. This strategy was used to noninvasively activate RGD peptide regions in vivo, and demonstrate increased cell adhesion, inflammation, fibrous encapsulation, and vascularization in uncaged regions.[32]

Click-type reactions provide an alternative method for postgelation patterning of hydrogels. Unlike radical photopolymerization, step-growth click polymerization reactions create homogenous networks, forming a uniform material for photopatterning.[33] Click reactions, including thiol-ene reactions, strain-promoted azide-alkyne cycloadditions (SPAAC), Diels–Alder ligation, and oxime/hydrazone formation have provided a range of strategies to surface pattern hydrogels.[34] In 2008, the Anseth group introduced a thiol-ene-based photopatterning approach exploiting mask-based photolithography; they independently patterned cysteine-based peptides into PEG-based networks formed through copper-catalyzed azide-alkyne cycloaddition (CuAAC) without affecting the physical properties of the gel.[35] The Bowman group demonstrated spatial and temporal control of the CuAAC reaction through a photochemical reduction of Cu(II) to Cu(I).[36] To avoid the need for a copper-based click reaction, DeForest et al. introduced an alternative thiol-ene click reaction patterning strategy with improved cytocompatibility using gels formed through a SPAAC.[37,38]

3D patterning of hydrogels has also been realized by integrating Diels–Alder click chemistry and thiol-ene reactions to biochemically pattern hydrogels.[39] Thiol-norbornene click reactions have been particularly popular for patterning hydrogels.[40–43] Fairbanks et al. first reported the use of a photoinitiated thiol-norbornene click reaction to pattern PEG hydrogels with peptides.[40] Building upon this, to incorporate both mechanical and biochemical gradients, a sliding mask was used to pattern thiol-norbornene hydrogels. These dual-gradient hydrogels were used to study elongation of human fibroblasts; it was found that keeping matrix stiffness or RGD density constant, while increasing the other, promoted human fibroblast spreading.[44] This technique has been expanded beyond PEG gels to sequentially pattern norbornene-functionalized HA (NorHA) hydrogels.[42,43,45] In one example, the extent of crosslinking of NorHA with dithiols was limited to allow for remaining pendent norbornene groups to react with thiol biomolecules.[42] Masks were used to create specific patterns and allowed for secondary patterning of nonfunctionalized areas.[42] Wade et al. coupled biochemical photopatterning of NorHA with topographical patterns created through electrospinning to investigate the effects of fibrous orientation and temporal biochemical modification on cell spreading.[46] Tetrazine–norbornene chemistry is another click reaction used to pattern hydrogels.[47,48] Alge et al. implemented a tetrazine–norbornene inverse-electron-demand Diels–Alder reaction to form PEG hydrogels, where pendent thiols could be photolithographically patterned with different norbornene-functionalized fluorescent bovine serum albumin (BSA) proteins.[47] Additional patterning chemistries used in conjunction with photomask lithography include aryl azide and allyloxycarbonyl reactions.[49–51]

Uncaging strategies have also been utilized to specify biomolecule binding to hydrogel surfaces. In one such strategy, Batt and co-workers exploited a photocleavable 2-nitrobenzyl group to liberate reactive carboxylic groups in patterns on a film, upon which proteins were subsequently conjugated through a reaction with their primary amine. The proteins' carboxylic acid moieties were then protected and the patterning was repeated through a photomask to sequentially immobilize additional proteins.[52] Alternatively, the DeForest group has developed and exploited a bioorthogonal photomediated oxime ligation strategy to immobilize proteins within cell-laden gels.[53–55] Here, a gel-bound alkoxyamine is photoliberated for subsequent reaction with aldehyde-modified proteins (Figure 3d).[54]

Selective hydrogel patterning of cells and proteins has also been achieved by adjusting the hydrophilicity of surfaces through photocleavage reactions.[56] Photoreleasable polymers utilizing *ortho*-nitrobenzyl (*o*NB) chemistry have also been used to control protein adhesion on hydrogel surfaces, by including an *o*NB group on nonfouling PEG brushes tethered to a polyacrylamide (PA) gel (Figure 3c).[57,58] Upon light exposure, PEG was removed in spatially defined regions, changing the exposed gel from noncell adhesive to cell adhesive. The precise geometry of the cell adhesive area was created through a photomask and secondary irradiation of the surrounding regions allowed cell migration to occur to the newly exposed cell-adhesive regions.

Subtractive Patterning: Light-triggered biochemical cue removal has also been demonstrated, whereby proteins, peptides, and DNA functionalized with a photocleavable group are photochemically released from hydrogels.[59–62] These strategies have been utilized to spatially control cell attachment, cytoskeletal organization, and ECM production. In one pioneering example, Kloxin et al. tethered RGD peptide to a PEG-based hydrogel through a photodegradable *o*NB ester-based linker; chondrogenic differentiation of human mesenchymal stem cells (hMSCs) was dictated through photochemical regulation

**ADVANCED
SCIENCE NEWS**
www.advancedsciencenews.com

**ADVANCED
MATERIALS
INTERFACES**
www.advmatinterfaces.de

of RGD presentation.[63] In order to further regulate protein release from hydrogels, Gawade et al. incorporated customizable, stimuli-labile linkers that allowed for user-defined control over hydrogel patterning; Boolean YES/OR/AND logic was used to release proteins by modifying the C-terminus with either single or multiple light, enzyme, or reductive sensitive moieties.[64] In one reported example, a protein functionalized with a photocleavable *o*NB and a reductive-sensitive linker placed in series was exposed to masked UV light to selectively pattern lines of protein and subsequently exposed to a reductant to fully release any remaining protein.

To circumvent the use of *o*NB-based linkers, Shadish et al. genetically fused a photocleavable protein (PhoCl) with a protein of interest to create protein-patterned gels using mask-based subtractive lithography.[65] Immobilized gradients of bioactive proteins (including growth factors) were obtained by adjusting the velocity by which an opaque photomask was translated over the gel. Alternatively, mask-based lithography can be used to initially spatially pattern biomolecules of interest, and a different release system can be employed to remove ligands on patterned areas. Zhang et al. capitalized on this concept by using thiol-ene click chemistry to selectively pattern DNA aptamers that captured complimentary proteins and were released by adding cDNA.[66,67] Sequential protein patterning was achieved by using a photomask to first pattern in an aptamer and the process was repeated with a separate aptamer. Independent protein release was controlled by adding the corresponding cDNA.[67]

Reversible Patterning: Although additive and subtractive patterning of hydrogels has been successfully utilized for cell culture platforms, the dynamic presentation of signaling biomolecules found in the ECM has sparked interest in the development of photoreversible patterning of hydrogels. DeForest and Anseth demonstrated photoreversible patterning of hydrogels by incorporating two bioorthogonal chemical reactions: a thiol-ene reaction for the incorporation of the biological molecule and a photolabile *o*NB group, to attach and subsequently remove cues in a PEG hydrogel network.[68] To establish dynamic control over cell function, NIH 3T3 cells were seeded on lines of photopatterned bioligands, where the initial attachment was confined; after secondary light exposure and removal of the adhesive ligand, cell detachment from the surface was observed.[68] In another photoreversible hydrogel system, DeForest and Tirrell introduced a photodeprotection-oxime ligation sequence for protein introduction and *o*NB photoscission for subsequent protein removal.[53] They demonstrated that osteogenic differentiation of hMSCs was confined in reversibly protein patterned 150 μm wide lines. Shadish et al. used a similar photorelease/oxime ligation sequence to immobilize site-specifically modified proteins while preserving their full bioactivity, creating Escher-inspired protein tessellations through masked photolithography.[54]

While the aforementioned techniques demonstrate improved mimicry of ECM presentation, the patterning and release of the molecule is not perfectly reversible as required functional groups are consumed during each patterning step. To overcome this limitation, the Anseth group introduced a reversible addition-fragmentation chain-transfer (RAFT) scheme using an allyl sulfide agent to pattern thiol-containing peptides and

proteins into hydrogel networks. This technique was used to demonstrate that reversible exchange reactions could be conducted in the presence of hMSCs.[69] In a follow-up work, Grim et al. incorporated a pendant allyl sulfide moiety onto a hydrogel backbone to allow for fully reversible and repeatable tethering of proteins through a photomediated thiol-ene click reaction.[70] This strategy was used to photoreversibly pattern TGF-*β*1 to induce localized cellular response in patterned areas, and upon release, return cells to an inactivated phenotype.[70] Surface hydrophilicity has also been reversibly altered for patterning. Wang et al. demonstrated photoreversible patterning of cells by using a photoresponsive hydrogel patterned with spiropyran units that responded to alternate visible–UV light irradiation, enabling a reversible hydrophobicity–hydrophilicity transition that stimulated the attachment and detachment of cells.[71] The use of light-sensing proteins (LSPs) has also been reported for light-activated reversible patterning of PEG hydrogels.[72,73] LOVTRAP, a two component LSP system, was recently used to spatiotemporally control noncovalent binding of recombinant proteins.[73]

3.1.2. Laser-Scanning Photolithography

Additive Patterning: In one of the earliest examples of additive biochemical gel patterning, a confocal-based scanning lithography method was developed for 2D and 3D surface patterning of PEGDA hydrogels.[74,75] Single-photon light was used to develop monolayered patterns of RGDS on PEGDA hydrogels for the spatially controlled attachment of human dermal fibroblasts (HDFBs).[74] SP-LSL has also been used for the patterned introduction of RGD and growth factors such as vascular endothelial growth factor (VEGF) to promote endothelial cell adhesion.[76] To develop more axially complex biochemical patterns, MP-LSL was used to generate patterned RGDS channels on collagenase-degradable PEG hydrogels to confine the migration of fibrosarcoma cells and guide the 3D migration of HDFBs (Figure 3a).[75,77] This technique was later expanded for micropatterning two fibronectin-derived peptides to demonstrate the effectiveness of MP-LSL for multi-step patterning of multiple peptides within the same hydrogel network.[78] MP-LSL has also been used to organize complex tubule networks of human umbilical vein endothelial cells (HUVECs) and 10T1/2s on RGDS-patterned hydrogels.[79]

To increase control of biochemical addition reactions, a photolabile protecting group can be added to temporarily mask functional groups. Luo and Shoichet modified agarose hydrogels with S-2-nitrobenzylcysteine as a photocaged thiol; UV irradiation triggered photocage release, exposing a free thiol that could be modified with RGD motifs to direct 3D growth of neural cells.[80] Wosnick and Shoichet replaced the nitrobenzyl photocage with a bromohydroxycoumarin thiol derivative; when exposed to femtosecond-pulsed near-infrared (NIR) light, two-photon-induced uncaging yielded 3D patterns with increased 3D resolution with low potential phototoxicity.[81] In later studies, coumarin-caged thiols were used to pattern gradients of human VEGF165 to guide endothelial cell growth, as well as for sequential protein immobilization based on the physical binding pairs, barnase–barstar and streptavidin

(SA)–biotin.[82,83] In further follow-up studies, this well-defined VEGF-gradient/GRGDS-immobilized agarose hydrogel was used to investigate interactions of endothelial cells and primary retinal stem and progenitor cells (RSPCs).[84] Owen et al. extended this photocaged patterning application to HA-based hydrogels and demonstrated independent control over biomolecule distribution, architecture topography and mechanical properties.[85] Hydrogels were prepared by reacting furan-modified HA with bis-maleimide–PEG. The biochemical density and mechanical properties were independently tuned by controlling the degree of furan substitution on the HA backbone.[85] HA hydrogel backbone modified with nitrodibenzofuran (NDBF) caged thiols have been patterned by MP-LSL to form gradients of endothelial growth factor (EGF).[86] EGF gradients differentially influenced breast cancer cell invasion and were used to demonstrate the importance of including cell–microenvironment interactions in examining cellular drug response.[86] Controlled laser light exposure has also been used to uncage the transglutaminase factor XIII enzyme and render it bioactive such that it could covalently tether a biomolecule of interest in highly localized, user-defined patterns.[87] Enzyme-mediated localized tethering of VEGF was used to direct mesenchymal stem cell outgrowth into a 3D patterned hydrogel.[87]

To avoid using UV light or pulsed NIR light, which could be damaging to cells and tissue at high doses, bromobimane has been used as a blue light-sensitive photocage for thiol groups on a PEG hydrogel.[88] Beyond using oNB, coumarin, and other small molecules as photocages, photoactivatable tris nitrilotriacetic acid (trisNTA) has been used as a photocage to selectively pattern biomolecular ligands.[89] Independent control of mechanical and biochemical properties using LSL has also been achieved with click reactions. DeForest and Anseth exploited wavelength-orthogonal photodegradation and photoaddition reactions to soften PEG hydrogels and incorporate adhesive ligands to guide cell migration.[90] Furthermore, a protocol for MP-LSL based on orthogonal enzymatic coupling and photocages allowed for the patterning of avidin-linked biotinylated growth factors (Figure 3b).[91] In the first step, a hydrogel containing caged peptides was formed in the presence of cells and biotinylated biological cues. After gelation, two-photon-based uncaging was performed using MP-LSL and enzyme-mediated ligation was then used to anchor nerve growth factor (NGF) in exposed areas. Using this system, the authors demonstrated axonal guidance of chick dorsal root ganglia (DRG) into areas of transglutaminase crosslinked hyaluronan matrix patterned with NGF. They found that Matrigel, collagen, and fibrin supported outgrowth whether or not NGF was present, and thus selected HA as the optimal matrix, since HA inhibited growth without the presence of NGF.[91] Methacrylated HA (MeHA) hydrogels patterned with adhesive peptides by MP-LSL have also been used to guide neurons.[92] Although chemical patterning alone was able to promote cell guidance, by combining chemical and mechanical cues, Seidlits et al. demonstrated the use of MP-LSL to separately control stiffness and adhesive ligand density on MeHA hydrogels.[92] Using this approach, they were able to guide both DRGs and hippocampal neural progenitor cells (NPCs) along defined 3D paths.[92] In another HA-based system, stiffness and matrix ligand density were systematically manipulated with distinct wavelengths of light to study nonlinear regulation of oncogenic microRNA by matrix stiffness and fibronectin density in glioma cells.[93] Wavelength-dependent patterning has also been employed to trigger stiffening of dextran–MA hydrogels with visible light, while UV light was used to photocleave DMNPB groups to activate an adhesive peptide at irradiated volumes.[94]

Subtractive Patterning: Subtractive patterning based on LSL can also be used to control the biochemical composition of hydrogels in 4D (i.e., in time and 3D space). Kloxin et al. incorporated a photolabile RGDS motif into a PEG hydrogel, and then removed the peptide in 3D patterns by using SP-LSL. The photolabile tether platform was used to control the differentiation of hMSCs into chondrocytes and used to demonstrate the importance of signal persistence on cell differentiation.[63] In addition to peptide release, digital maskless photolithography has been used to liberate oligonucleotides from DNA-functionalized PEGDA hydrogels. Visible light was initially used to polymerize PEGDA hydrogels into a variety of shapes and multidomain structures that contained different DNA molecules; UV light was then used to selectively cleave DNA oligonucleotides containing a cleavable linker in their backbone.[95] In a more recent report, Shadish et al. incorporated proteins into a hydrogel through a linker containing the photocleavable protein, PhoCl, with an azide attached to the N-terminus, to conjugate into PEG hydrogels through a SPAAC reaction; SP-LSL was then used to release the protein and pattern different proteins of interest.[65]

Reversible Patterning: MP-LSL has also been used to reversibly control biochemical cue presentation. DeForest and Tirrell used MP-LSL for 3D control over protein immobilization and demonstrated photoreversible immobilization of proteins.[53] They used a SPAAC reaction for network formation, a photodeprotection-oxime-ligation sequence for protein introduction, and an oNB photoscission reaction for protein removal; removal of protein patterns was controlled in 3D by varying the multiphoton laser-scanning conditions which allowed for complex dual-protein patterning.[53] In a similar set up, MP-LSL was used to create trifunctional protein patterns in 3D space. Initially, a fluorescent protein was immobilized into a SPAAC-based gel through photomediated oxime ligation. Proteins were then released through oNB cleavage. Areas of photorelease could be backfilled by a second and third fluorescent protein of interest (Figure 3d).[54] Additionally, allyl sulfide chemistry has been utilized to reversibly tether proteins into gels by MP-LSL.[70] Although both mask-based and LSL patterning techniques have been employed to reversibly immobilize biochemical cues, improvements in chemistries and better on demand modulation will aid in recreating dynamic cellular microenvironments.

3.2. Soft Lithography

Soft lithography has seen a rise in popularity since the Whitesides group first demonstrated agarose stamps could be used to pattern gradients of proteins onto hard surfaces such as silicon or glass.[96] Since these hard surfaces are not representative of the cellular microenvironment, research turned toward developing microcontact printing techniques compatible with softer

**ADVANCED
SCIENCE NEWS**
www.advancedsciencenews.com

**ADVANCED
MATERIALS
INTERFACES**
www.advmatinterfaces.de

surfaces, such as hydrogels. Unfortunately, due to their soft and tacky nature, typical hydrogels cannot withstand the strong physical pressure needed to transfer patterns and are not amenable to conventional μCP of biomolecules from PDMS. Thus, several methods have been developed to circumvent sticking and to improve patterning using PDMS stamps, including chemical modification of hydrogels, sequential delivery, and freeze drying.[17,97]

Burnham et al. first reported a chemical modification method to functionalize hydrogels with biological molecules by μCP for cell culture studies.[97] A PDMS stamp containing PEO-iodoacetyl biotin was initially placed on a hydrogel coating containing free disulfides. The hydrogel was then incubated with SA, which could bind additional biotinylated molecules conjugated to proteins. To pattern in a second protein after the first pattern of SA had been applied, the hydrogel was either immersed in 1) PEO-iodoacetyl biotin to fill in unstamped areas containing unreacted thiol groups that could be incubated to react with a second protein, or 2) a fresh PEO-iodacetyl biotin stamp was applied for repeated rounds of μCP.[97] This technique was then used to immobilize multiple proteins and peptides, including biotinylated fibronectin, laminin, and an adhesive peptide ligand (i.e., biotin-IKVAV), for the controlled growth of neural cells.[98] A separate work studied selective adhesion and neurite extension and formation of synapses of rat astroglial and primary hippocampal neurons on fibronectin and laminin patterned areas by μCP.[99] In another chemical modification technique, Grevesse et al. demonstrated that patterning by μCP controlled ligand density on hydroxy-PA gels without affecting stiffness, which was regulated by varying the crosslinker concentrations. HUVEC spreading and morphology was confined to areas of fibronectin-coated micropatterns.[100] μCP has also been used to pattern biochemical ligands on PA hydrogels chemically treated with hydrazine to study MSC lineage specification.[101]

Rather than chemically altering the hydrogel surface, Lee et al. modified PDMS stamps with polydopamine (PD) which has been shown to undergo self-polymerization on surfaces and easily bind proteins; they found that HDFBs adhered preferentially to PD-bound BSA patterns.[102] In another procedure coined nanocontact deprinting, Au nanoparticles (NPs) were transferred from a solid silicon surface to a PEG-based hydrogel.[103] A PDMS stamp was first functionalized with a self-assembled monolayer of amino-silane that was subsequently decorated with citrate-capped Au NPs via electrostatic interactions. The stamp was then brought into contact with the PEG hydrogel and, depending on the chemical functionality of the gel surface, the Au NPs were transferred. Stamping on nonfunctionalized PEG hydrogel surfaces required a larger amount of force to transfer the Au NPs onto its surface, while on thiol-functionalized PEG hydrogel surfaces, light contact was sufficient for efficient transfer. This technique was used to demonstrate preferential cell adhesion of murine fibroblast L929 cells on the patterned areas.[104] To overcome the constraints of chemical modifications, such as the multiple required steps, a simple method involving freeze-drying a Matrigel hydrogel prior to printing was proposed. PDMS stamps were then used to transfer streptavidin, laminin, and fibronectin proteins through physical adsorption to the lyophilized hydrogel. Using this

technique, the authors demonstrated that human embryonic stem cells (ESC) cultured on fibronectin-patterned hydrogels displayed beating foci earlier than those cultured on nonpatterned substrates.[17]

PDMS stamps may adhere to a hydrogel and cause substrate deformation.[105] Thus, as an alternative to PDMS stamps, Di Benedetto et al. used Parylene C to pattern PEGDA hydrogels.[106] Parylene C is preferred for patterning PEGDA hydrogels for two reasons: 1) Parylene C mold preparation does not require as extensive or complicated microfabrication steps, and 2) Parylene C has lower oxygen permeability than PDMS. Sanzari et al. used this general method to study the cell morphology and physiology of collagen patterns on neonatal rat ventricular myocytes. They observed cell elongation and alignment within collagen-patterned areas.[107,108] In another example, 5 to 400 μm wide lines of fibronectin, laminin, and collagen I were patterned onto PA gels.[109] Normal fibroblasts cultured on patterned areas of the gel surface showed enhanced cell attachment and proliferation confined within the boundaries of the pattern.[109]

3.3. Electron-Beam Lithography

E-beam lithography has been primarily used to immobilize biomolecules in hydrogels by increasing the hydrophobicity or functionality of a polymer. E-beam lithography for generating multicomponent protein patterns was first reported by the Maynard group. A PEG polymer was modified with four protein-reactive moieties: biotin, maleimide, aminooxy, or Ni^{2+}-NTA, which could then react with its corresponding substrate. When PEG is exposed to electron beams, it crosslinks as well as reacts with Si surfaces in a manner similar to radical-mediated crosslinking. To demonstrate multiprotein patterning, they developed tricomponent biostructures by first crosslinking biotin PEG polymer spin coated on a Si wafer. Next, they created two 1 μm wide maleimide–PEG and 1 μm wide aminooxy–PEG patterns on the biotin–PEG pattern, and finally, they conjugated the corresponding fluorescent proteins.[110] Using a similar method, but employing click chemistry, α-ketoamide–myoglobin followed by azide-modified ubiquitin were conjugated to a hydrogel surface to form dual multilayer click protein patterns.[111] Rather than using e-beam lithography for creating consecutive layers, the technique has also been used to encapsulate a protein immobilized hydrogel inside another hydrogel with features ranging from 5 to 40 μm. The enzyme glucose oxidase (GOx) was immobilized in the core shell and horseradish peroxidase was conjugated to the shell periphery, where bioactivity was demonstrated through enzyme cascade reactions.[112]

3.4. Inkjet Printing-Based Patterning

Inkjet bioprinting, developed by Thomas Boland, has proven to be an attractive technique to create complex patterns on hydrogels without the need to fabricate masks.[113,114] In early studies, thermal inkjet printing was demonstrated to be a feasible method to pattern gradients of cells, including Chinese

hamster ovary (CHO) cells, embryonic motoneuron cells, primary neurons, and mesodermal stem cells onto collagen hydrogels while still maintaining their viability and differentiation potential.[115,116] To show that this technique could control neural stem cell (NSC) multipotency and differentiation, Ilkhanizad et al. used an inkjet printer to print gradients of biologically active macromolecules on PA hydrogels; they were able to grade differentiation of NSCs cultured on areas printed with ciliary neurotrophic factor (CNTF), where cells displayed the highest levels of differentiation markers at the edge of the hydrogel with the highest concentration of CNTF.[20] Gurkan et al. demonstrated control over differentiation of MSCs into osteogenic and chondrogenic phenotypes by developing a biochemical gradient through bioprinting nanoliter droplets encapsulating human MSCs, bone morphogenetic protein 2 (BMP-2), and transforming growth factor-β1 (TGF-β1), to create an anisotropic biomimetic fibrocartilage microenvironment.[117] In a more recent example, inkjet printing was used to develop a high-throughput assay format for printing enzyme-immobilizing/stabilizing hydrogel microarrays to predict IC50 values of inhibitors.[118]

Other similar techniques to inkjet printing include extrusion-based bioprinting and electro-hydrodynamic jet (e-jet) printing. By using extrusion bioprinting, Fedorovich et al. spatially patterned cells in a variety of hydrogels and showed that cell viability was influenced by the hydrogel employed during cell printing.[119] E-jet printing is another effective process for patterning hydrogels: ink is placed in a sealed reservoir with a conductive nozzle and upon applying a capillary force and a potential difference between the nozzle and hydrogel surface, an electric field is created that pulls fluid out.[120] The droplet size and jetting frequency depend on the back-pressure, the separation distance between nozzle and the hydrogel substrate, and the applied voltage.[120] Like inkjet bioprinting, patterning by e-jet printing can be controlled at the point of printing without the need of fabricating stamps or masks. Poellman et al. first applied e-jet printing onto a soft surface by printing fibronectin on a PA hydrogel and demonstrated cell attachment and spreading on patterned areas.[120]

3.5. Controlled Mixing and Microfluidic Patterning

Simple biomolecular gradients can also be generated using gradient makers.[121,122] DeLong et al. generated a gradient of basic fibroblast growth factor (bFGF) by using a gradient maker to pour a precursor monomer solution and then photopolymerizing the solution to obtain a hydrogel with a concentration gradient. Cells aligned in the direction of increasing bFGF and vascular smooth muscle cells (VSMCs) migrated differentially toward the direction of increasing bFGF.[121]

Microfluidic techniques have also enabled precise control over the spatial distribution of biochemical signals on and within 3D scaffolds, particularly for fabricating graded biomolecular patterns (**Figure 4**). Burdick et al. introduced a method to fabricate patterns of RGDS on PEGDA hydrogels by combining microfluidics and photopolymerization; gradients of the photo-crosslinkable monomers were formed within microfluidic channels and subsequently gelled by exposure to UV light, resulting in increased endothelial cell adhesion in areas with higher concentrations of RGD.[123] Simple PDMS microfluidic gradient generators have also been used to fabricate linear concentration profiles of immobilized RGD peptide in a photopolymerizable PEGDA hydrogel to study the effects on rat MSCs adhesion (Figure 4a). Actin staining showed that at high RGD concentrations, MSCs showed good spreading morphology, whereas at low RGD concentration regions, MSCs displayed a rounded shape.[124] To generate PEGDA hydrogels with both mechanical and biochemical gradients, Turturro and Papavasiliou employed a free-radical photopolymerization technique to selectively deliver eosin Y photoinitiator that generated a wave-like local reaction zone that propagated through a monomeric solution; through a gradient of immobilized YRGDS, they directed fibroblast cell behavior.[125] Rather than using photopolymerization to generate gradients, hydrodynamic flow focusing has been used to capture in a step-wise manner tagged biomolecules via affinity binding onto functionalized PEG hydrogel surfaces (Figure 4b).[126] The microfluidic device allowed for the orthogonal and parallel patterning of four proteins. By rotating the microfluidic device 90°, they were able to pattern a second row of parallel protein gradients. This system was used to study how leukemia inhibitory factor (LIF) influenced ESC behavior.[126]

Rather than immobilizing biochemical signals, microfluidic devices can also be used to generate soluble, diffusion-driven concentration gradients in 3D cell-embedded hydrogels (Figure 4c).[127] These 3D hydrogel-based microfluidic devices have been used to study hMSC chemotaxis and chemokinesis, fibroblast and osteoblast migration, and for anticancer drug screening.[128–131] Microfluidic devices have also been used to demonstrate independent control over chemical and mechanical gradients (Figure 4d).[132] The microfluidic device was used to generate a gradient of hepatocyte growth factor and show that cell velocity was dependent on both mechanical and biochemical cues.[132]

3.6. Additional Techniques

Although the techniques described above are the most common routes for biochemical patterning of hydrogel surfaces, additional methods have been reported. Kramperman et al. introduced an interesting strategy for spatially controlled hydrogel modification through diffusion-mediated competitive supramolecular complexation. Specifically, a dextran-based hydrogel with biotin (DexTAB) available for postfunctionalization was used for competitive supramolecular functionalization to create gradients by controlling the penetration depth of biotinylated moieties. Multistep modification of Dex-TAB in the presence of live reporter cells demonstrated that the supramolecular desthiobiotin/biotin displacement strategy could provide biotinylated hydrogels with temporally controlled biochemical cues to instruct cell behavior.[133] In another diffusion-controlled technique, radially patterned hydrogel channels were fabricated via the sequential injection of crosslinkers containing bioorthogonal capping groups which enabled the spatial patterning of vascular cells, and demonstrated an initial step toward engineering implantable arteries.[134] Dicker et al. spatially patterned biochemical cues in a core–shell fashion using an interfacial
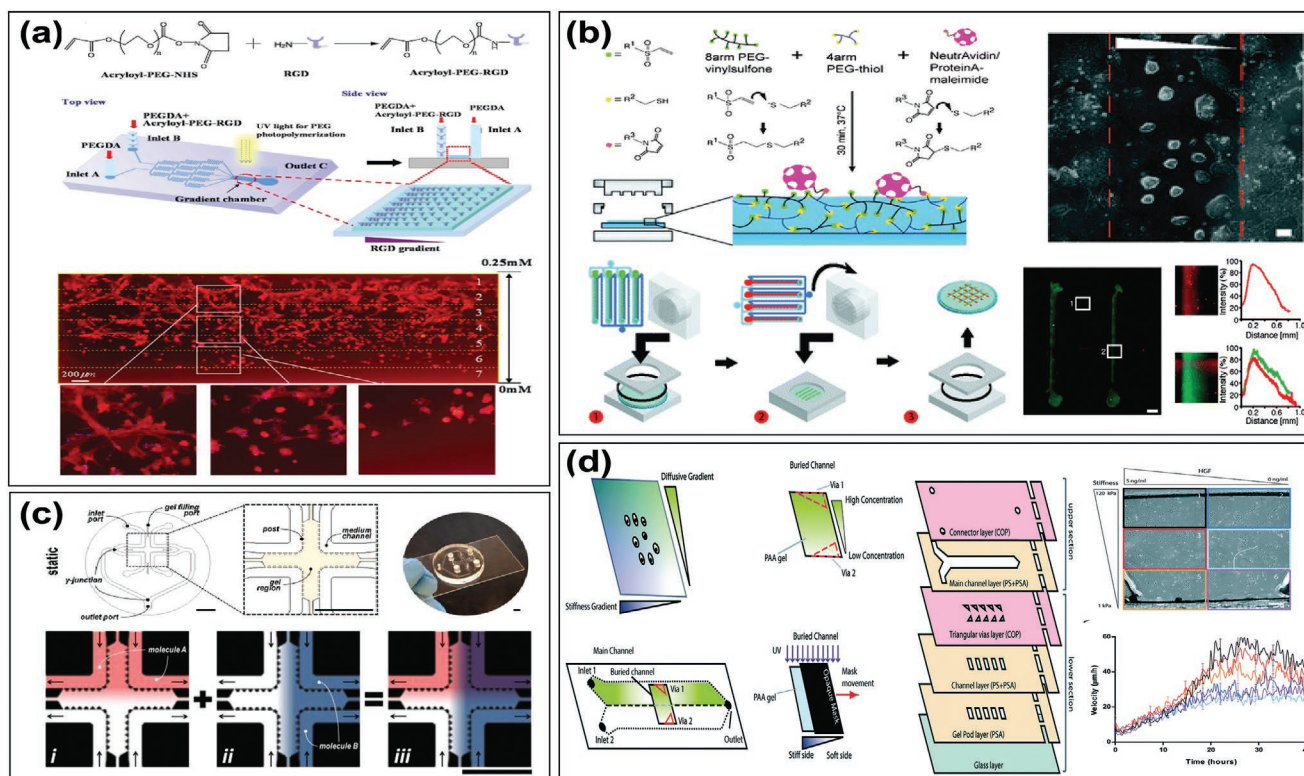
**ADVANCED
SCIENCE NEWS**

www.advancedsciencenews.com

**ADVANCED
MATERIALS
INTERFACES**

www.advmatinterfaces.de

Figure 4. Biochemical patterning of gel surfaces through microfluidic methodologies. a) Top: formation of PEG hydrogel containing graded RGD using microfluidic gradient generator. Bottom: Gradient distribution of cell spreading on PEG hydrogel. Reproduced with permission.[124] Copyright 2012, American Institute of Physics. b) Hydrogel patterning via protein capture by flow focusing. Top: Schematic of bioconjugation method and ESC spreading on a LIF protein gradient. Bottom: Scheme showing patterning of arrays of overlapping gradients and micrographs of fluorescent protein gradients generated. Scale bar = 900 μm. Reproduced with permission.[126] Copyright 2013, Royal Society of Chemistry. c) Microfluidic design of an orthogonal gradient generator. Reproduced with permission.[127] Copyright 2015, Wiley-VCH. d) Left: Generation of diffuse chemical gradient independent of substrate stiffness gradient. Right: Device validation using hepatocyte growth factor scattering assay and time evolution of cell velocity. Reproduced with permission.[132] Copyright 2015, Royal Society of Chemistry.

tetrazine ligation by altering the composition of the crosslinking solution.[135] In another controlled reaction pattern formed by diffusion, the diffusion term of the system was tuned to generate a DNA pattern in an alginate gel containing immobilized PA. In an associative toehold activation type reaction, which can capture an input if both inputs exist, a DNA logic AND gate was anchored in the gel to detect the diffusion of molecules from distant source points to produce a Voronoi pattern in the gel. The proposed framework would be useful in designing a structured gel system responsive to molecular signals.[136]

To overcome the limited resolution of bioprinting (180 μm), a noncontact method for specifying cell alignment where cells align along the nodes or antinodes of the acoustic field—acoustophoresis—has been used to generate patterns.[137,138] This method was employed to direct the assembly of myoblasts in collagen hydrogels, stimulate the cells to undergo myogenesis, and thus, engineer bundles of aligned myotubes.[137] Ma et al. also employed this technique to project a complex shape into a cell suspension flow, which caused cells to move and aggregate at the high acoustic pressure zones and form 2D patterns on a collagen solution. Subsequent gelation was employed to immobilize the cell patterns in a 3D matrix.[138]

As an alternative to light dependent reactions, an enzyme-mediated polymerization reaction, using GOx to generate hydrogen peroxide that can react with ferrous ions to produce hydroxyl radicals, was carried out on the surface of a hydrogel to spatially control the formation of 3D hydrogel layers and incorporation of rhodamine-B, fluorescein, and different sized nanoparticles.[139] Combining this enzyme-mediated patterning technique with other approaches such as photolithography could prove advantageous for tissue engineering applications.

4. Mechanical Patterning of Hydrogel Substrates

Cells in multicellular tissues experience compressive, tensile, and shear forces, all of which play a critical role in the assembly, development, and maintenance of tissue.[140] In particular, research has focused on modulating the most accessible and easily tunable mechanical feature of materials: stiffness, otherwise termed the elastic modulus. The elastic modulus is defined as the ratio of force exerted upon a material to the resulting deformation.[2] By specifying the method and direction stress and strain are applied and measured, a variety of elastic moduli can be defined; for instance, Young's modulus (E) is calculated by subjecting a material to uniaxial stress (either compressive or tensile) and measuring the elastic (reversible) deformation (strain). The shear modulus (G) is similarly calculated, however,

**ADVANCED
SCIENCE NEWS**

www.advancedsciencenews.com

**ADVANCED
MATERIALS
INTERFACES**

www.advmatinterfaces.de

the stress and deformation are parallel and associated with an angular change.[2] Young's moduli for tissues range from hundreds of pascals of neural tissue to tens of gigapascals for bone.[3]

Numerous studies have implicated the role of stiffness of the ECM in altering cellular adhesion structures, motile behavior, and proliferation.[141–145] Furthermore, naïve MSCs specify lineage and commit to phenotypes based on matrix elasticity; as an example, softer (0.1–1 kPa) substrates mimicking the brain are neurogenic, mid-range (8–17 kPa) substrates are myogenic, and stiffer (25–40 kPa) substrates are osteogenic.[146] Yet tissue is viscoelastic, meaning that part of the deformation to stress is nonreversible (plastic). As such, the shear or elastic modulus has two components: 1) a storage modulus (G', E') denoting the elastic contributions, and 2) the loss modulus (G'', E'') denoting the plastic contributions. Recently, tuning of viscoelasticity has been shown to influence cellular spreading, proliferation, and stem cell fate.[147–149]

Despite the vast body of scientific knowledge, the molecular basis of mechanotransduction remains relatively unclear. It is generally accepted that mechanical signals from the ECM are sensed through focal adhesion (FA) assemblies, or integrin clusters that form a link between intracellular actin bundles and the ECM, which are transduced via the actin cytoskeleton network. In passive sensing, cells exert traction forces on the ECM and following a cascade of FA assembly, Rho activation, and actomyosin contraction, cells gauge the resistance of the substrate.[150] Other transcription factors such as yes-associated protein (YAP) and transcriptional Co-activator with PDZ-binding motif (TAZ) have been shown to localize to the nucleus in response to stiffening events and mediate the apoptosis, proliferation, and differentiation of MSCs.[151] In active sensing of ECM mechanics other mechanisms such as mechanically gated ion channels and direct transmission of force to the nucleus have been implicated.[152,153]

Cells interact with various mechanical cues, ranging from the magnitude of ECM proteins, to bulk tissue.[2] To accurately capture the extent and heterogeneity of elastic moduli for studying mechanosensitive phenomena and recapitulating the in vivo cellular environment, biomaterials must be designed with spatial distribution of mechanical cues. In a covalently crosslinked network, this is readily achieved by varying the crosslink density.[33] This section details various techniques to achieve spatial control over elastic modulus and, less commonly, viscoelasticity.

4.1. Controlled Mixing

One of the most facile yet powerful techniques to establish defined gradient patterns in hydrogels is through controlled mixing of solutions of varying crosslinker or monomer weight percentage. While the most basic implementation of controlled mixing is by coalescing two droplets of prepolymer in between glass coverslips, this offers limited user control over gradient patterning. Thus, more advanced approaches such as microfluidic devices and gradient mixers have provided increased command over gradient development. This principle, due to its simplicity, is accessible to researchers outside of the biomaterials community intending to study biological mechanotransduction phenomena.

4.1.1. Coalescing of Prepolymer Solutions

By the start of the 21st century, it had been shown that cells responded differently to stiffer substrates, but no studies had been able to demonstrate how cells reacted to spatially distributed elastic moduli.[141] Lo et al. introduced the concept of "durotaxis;" in their seminal study, they created a gradient of Young's moduli in PA gels by varying bis-acrylamide concentrations in two adjacent drops and observed fibroblast migration to stiffer surfaces. They hypothesized that as the leading edge of the cell crosses onto a stiffer substrate, this causes the lamellipodia to protrude, leading to directed migration.[154] Since this initial study, improved methods for generating more controlled stiffness gradients in PA have been proposed. For instance, a dumbbell-shaped mold in between glass slides of differing hydrophobicity enabled controlled mixing of the two prepolymer solutions to create stiffness gradients ranging from ≈3 to ≈72 kPa mm^{-1}.[155,156] Hadden et al. proposed a simple stiffness gradient platform: an initial aliquot of a defined acrylamide monomer concentration was poured into a mold and covered with a glass coverslip so that the polymerization chamber assumed a right-angled ramp. A second solution of acrylamide monomer was poured in following the initial reaction, and polymerized to form a layered pair of inversely oriented ramps with a range of stiffnesses. By changing the ramp angle, they created shallower and steeper stiffness gradients. They explored different linear stiffness gradients and demonstrated that 2.9 kPa mm^{-1} was not durotactic for human adipose derived stem cells (hASCs), enabling studies of more subtle, dose-dependent responses to mechanical cues (**Figure 5**a).[157]

Similar studies have been done in PEG-based hydrogels. Peristaltic pumps have been used to create more defined gradients in PEGDA and PEG–dimethacrylate (PEGDMA).[158,159] Chatterjee et al. created a compressive modulus gradient ranging from 12 to 306 kPa and induced graded osteogenesis and mineralization in the absence of any other biochemical cues, underscoring the importance of mechanical cues in cellular differentiation (Figure 5b).[159]

4.1.2. Microfluidic Patterning

Microfluidic channels have emerged as a more advanced solution for generating gradients, as they provide precise control over stiffness at the micrometer length scale and easier manipulation of gradient intensity.[160–162] In PA, gradients of elastic modulus ranging from 3 to 40 and 5 to 80 kPa have been used to study VSMC spreading and motile response.[163,164] Vincent et al. sought to understand the response of MSCs to different tissue variations by utilizing three techniques (soft lithography, microfluidics, and photomasking) to achieve step (100 Pa μm^{-1}), pathological gradient (10–40 Pa μm^{-1}), and physiological gradient (≈1 Pa μm^{-1}) changes in elastic modulus. MSC durotactic speed correlated with gradient strength. Upon blocking of microtubule and cytoskeleton assembly, cells exhibited inhibited cell polarity and reduced spread area, implying that these two components are critical for transmitting forces to and probing the surrounding environment (Figure 5c).[162] PEGDA has also been demonstrated as an amenable polymer system for microfluidic patterning.[160,165]
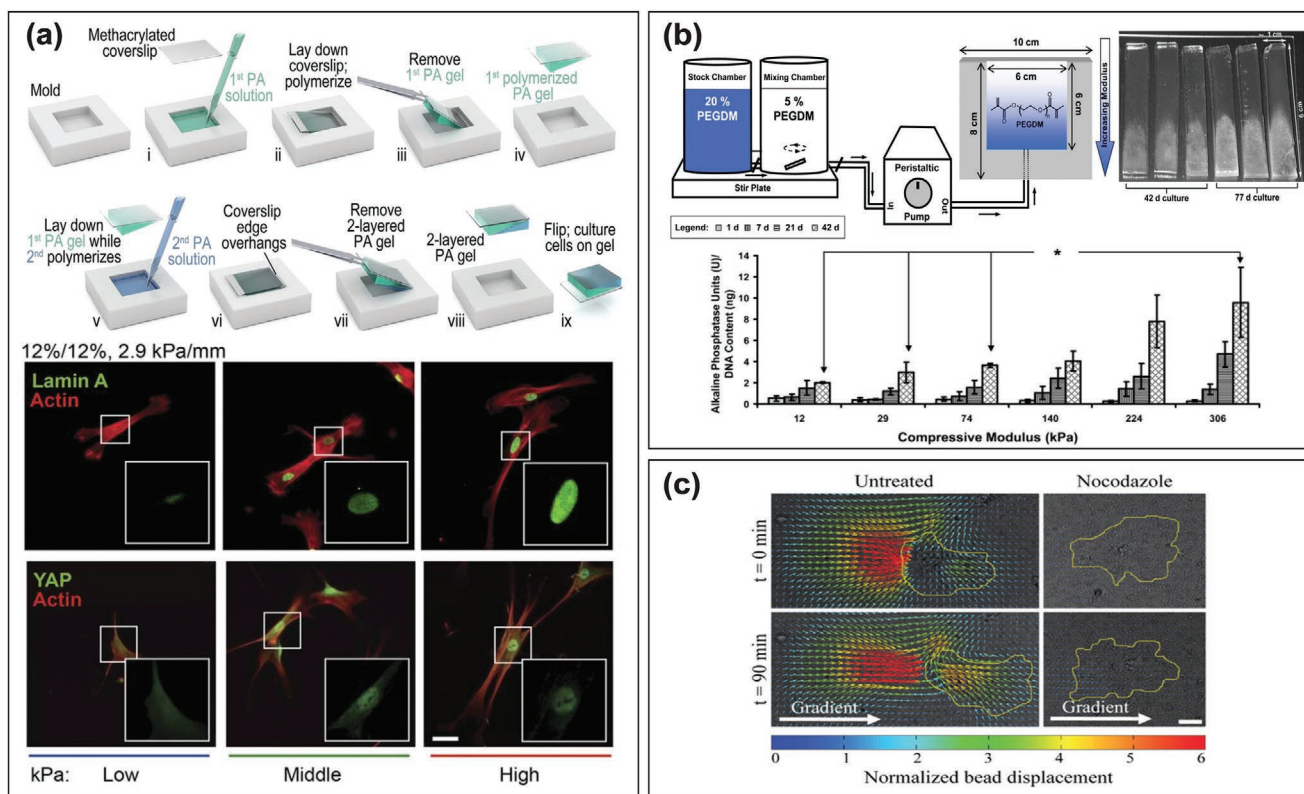
**ADVANCED
SCIENCE NEWS**

www.advancedsciencenews.com

**ADVANCED
MATERIALS
INTERFACES**

www.advmatinterfaces.de

Figure 5. Examples of controlled mixing to pattern mechanical cues. a) Hadden et al. developed a method (top) to pattern more defined gradients using a ramp-based mold, enabling them to examine expression of proteins (bottom) such as Lamin A and YAP at small gradients that do not elicit durotaxis. Reproduced with permission.[157] Copyright 2017, National Academy of Sciences. b) Top left: PEGDMA gels with gradients of elastic moduli are made with a gradient mixer. Top right and bottom: The degree of expression of osteogenic markers such as alkaline phosphatase can be controlled by solely a mechanical gradient. Reproduced with permission.[159] Copyright 2010, Elsevier Ltd. c) Vincent et al. demonstrated that blocking actin assembly with nocodazole disables cell movement, even in the presence of a gradient generated by a microfluidic device. Reproduced with permission.[162] Copyright 2013, Wiley-VCH.

Forming stiff gels with microfluidic patterning may be difficult, as the PDMS channel material is porous and allows molecular oxygen to diffuse through that can interfere with the polymerization reaction. However, this effect can be counteracted with different surface coatings.[162]

4.2. Photolithography

Photolithography has emerged as a potent tool for patterning elastic modulus and other mechanical cues in hydrogel systems. Photopolymerization chemistries, particularly acrylate and acrylamide polymerizations, have been utilized to generate gels with spatially defined crosslinking densities. Conversely, others have focused on developing photosoftening systems based on *o*NB groups and other photosensitive moieties, whereby light exposure directs crosslink scission.

4.2.1. Mask-Based Photolithography

Mask-based lithography has gained popularity as a simple, spatially defined technique for creating gradients or other geometric patterns of elastic moduli. Masks can be used to control

the degree of light exposure; by exposing certain regions of photopolymerizable substrates to more light, a more stiffer region with higher crosslinking density is generated. Inversely, with photolabile chemistries, exposed crosslinks can be degraded, leaving an area with a lower elastic modulus compared to the unexposed area.

Photostiffened Patterning: As with controlled mixing, many of the initial advances in mask-based lithography were in PA. Early work by Wong et al. demonstrated that during photopolymerization, grayscale radial gradient patterns could be used to generate substrates with gradients in mechanical compliance to guide vascular smooth muscle cell migration.[166] Others have used similarly graded masks to discern how the steepness of the gradient affects MSC durotaxis.[5] Gradients have also been generated by moving a mask with variable speed over prepolymer solution.[44,167] More complex patterns, such as alternating lines of different elastic moduli, have been accomplished by employing a dual-step polymerization technique, whereby the initial hydrogel is soaked in a second acrylamide monomer solution, which can be selectively crosslinked in user-defined patterns. Such approaches have been used to spatially control co-cultures of myoblasts and motor neurons.[168]

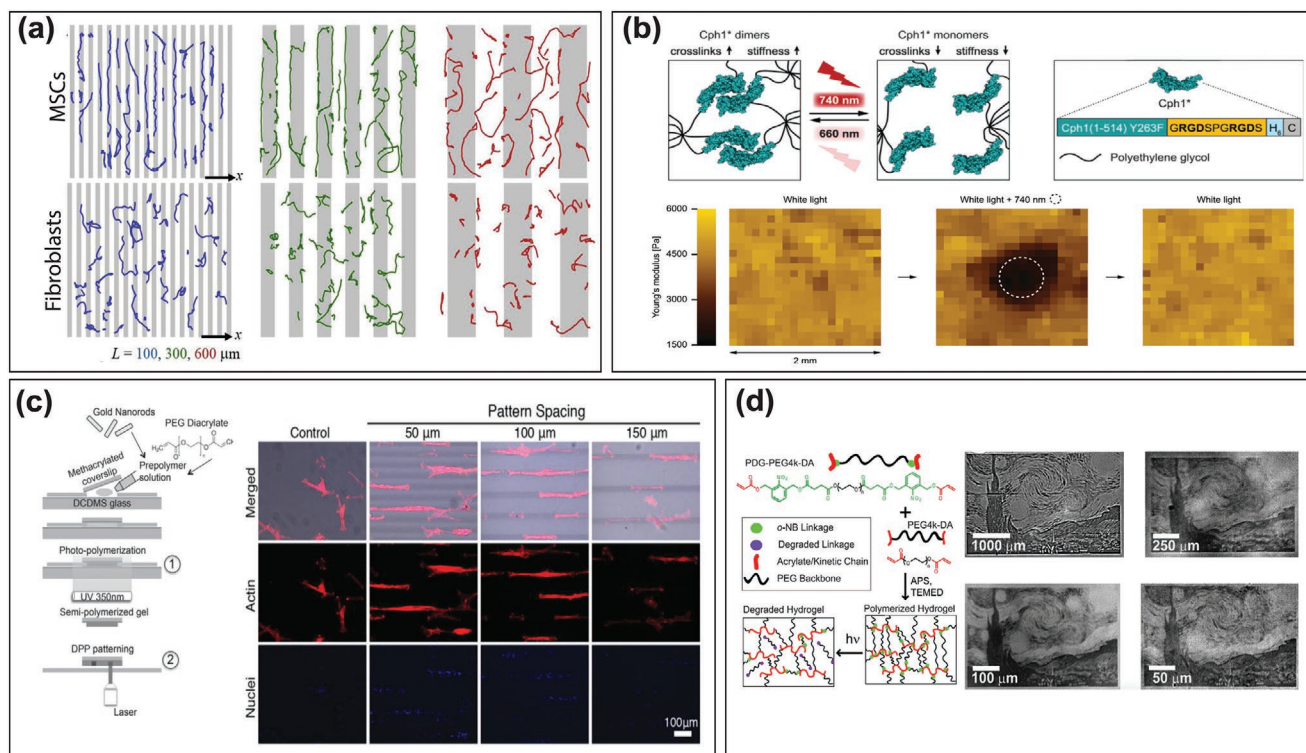As an alternative to PA, styrenated gelatin has also been patterned by a two-step process with a digitally projected

**ADVANCED
SCIENCE NEWS**
www.advancedsciencenews.com

**ADVANCED
MATERIALS
INTERFACES**
www.advmatinterfaces.de

Figure 6. Photolithographic patterning of elastic modulus. a) Patterned styrenated gelatin with lines of different widths induces different cell movement. Reproduced with permission.[173] Copyright 2020, Elsevier Ltd. b) The Cph1 system for reversible mechanical patterning with 740 nm light. Reproduced with permission.[95] Copyright 2019, Wiley-VCH. c) NIR photostiffening of PEGDA (left) with gold nanorods guides SMC spreading and localization (right). Reproduced with permission.[200] Copyright 2014, Wiley-VCH. d) Photodegradable PEGDA crosslinkers are used to generate grayscale patterns of elastic modulus. Reproduced with permission.[204] Copyright 2016, American Chemical Society.

photomask. Gradients, step changes, and more complex patterns helped elucidate the elastic gradient threshold for durotaxis of fibroblasts and MSCs, as well as propel movement along one axis.[169–172] Building upon this, Ebata et al. examined the effect of unit width (ranging from 100 to 600 µm) of stiffer regions on cellular durotaxis and demonstrated that specific cell types accumulate preferentially in different width lines, potentially mimicking in vivo spontaneous aggregation of different cell types in regions of varied elastic moduli (**Figure 6**a).[173]

While PA and styrenated gelatin have been critical for answering fundamental questions about cellular movement and differentiation, they cannot be translated into 3D applications due to the cytotoxicity of the polymerization conditions. The concept of increased crosslinking in defined regions has been employed with more cytocompatible chemistries, such as free-radical polymerization of acrylates and methacrylates.[174] Nemir et al. patterned PEGDA gels via a two-step process to achieve stripes and grids with less-crosslinked regions (elastic moduli ≈3.4 kPa) and more-crosslinked regions (elastic moduli ≈20 kPa) to study macrophage migration.[158] Marklein and Burdick introduced the first use of sequential crosslinking of MeHA with sliding or geometrically patterned masks to create elastic moduli ranging from 6 to 25 kPa.[175] Subsequent studies in MeHA investigated hMSC spreading, hepatic stellate cell differentiation, and chick aortic arch growth in response to patterned step changes in elastic modulus.[176–178]

Thiol-ene photoclick reactions have also been employed for patterning mechanical cues in both natural and synthetic hydrogels. Petrou et al. functionalized digested porcine lung ECM with thiol groups to crosslink with PEG-α-methacrylate and demonstrated that fibroblasts upregulated αSMA and Col1A1 expression on stiffer, fibrotic tissue-mimicking regions ($E = 14$ kPa) as compared to on softer, healthy tissue regions ($E = 5$ kPa).[179] Furthermore, norbornene groups have been added to HA and PEG, providing a reactive handle for photochemical modulation.[180,181] Of note, Hui et al. gained the ability to pattern changes in material viscoelasticity by modifying a covalently crosslinkable NorHA network with cyclodextrin and adamantane supramolecular crosslinks. Using a photomask, they created hydrogels with stiff, elastic areas, surrounded by soft, viscoelastic regions to mimic the heterogeneous fibrotic environment.[180] Other patternable, photostiffening PEG systems, based on photocaging of alkoxyamines and photocyclodimerizing anthracene moieties, have also been demonstrated to be cytocompatible and able to activate fibroblasts.[182,183]

Photosoftened Patterning: Using similar concepts found in biochemical patterning, photomasks can be used to "subtract" elastic modulus in defined regions through selective exposure of photolabile crosslinks to light. Many systems are based on the photodegradable *o*NB functional group. In one of the first instances of spatially controlled softening, PA was activated with hydrazine hydrate to create polyacrylamide acryl hydrate, which could be crosslinked with 4-bromomethyl-3-nitrobenzoic

**ADVANCED
SCIENCE NEWS**
www.advancedsciencenews.com

**ADVANCED
MATERIALS
INTERFACES**
www.advmatinterfaces.de

acid. The crosslinker's photolysis rate at $\lambda = 365$ nm was dependent upon the energy of illumination; softening the gel from 7.2 ± 0.8 to 5.5 ± 0.1 kPa in anterior regions of NIH 3T3 cells elicited a dramatic shift or loss in cell polarity.[184] Kloxin et al. followed suit with an influential series of reports on a novel, oNB incorporating, PEG–di(photodegradable acrylate) (PEGdiPDA) crosslinker that could react with PEGDA.[63,185–187] Specifically with mask-based lithography, Kloxin et al. utilized this system to pattern gradients and geometric shapes, with previously described sliding masks and cut-out patterns, to screen the influence of substrate elasticity on hMSC spreading, as well as determine the threshold deactivation modulus of valvular interstitial cells (VIC).[186,187]

Subsequent studies elaborated on this chemistry for patterning applications. Xue et al. described a dual-tone system of swollen or eroded topographic patterns, superimposed on a pattern of elastic modulus, whereby varying the exposure time controlled the extent of crosslink degradation.[188] The oNB moiety has also been incorporated into N-hydroxysuccinimide-terminated-photocleavable PEG and methacrylated-photocleavable-gelatin.[189,190] PEGdiPDA has since been used to study the effect of organized and randomly arranged patterns of elastic moduli on hMSC and VIC differentiation and activation.[191,192]

Protein-Based and Reversible Stiffening Systems: Recent interest in the area of protein engineering as well as innovations in the optogenetic space have led to the development of novel hydrogels based on protein crosslinkers to modulate elastic modulus. Xiang et al. created photosoftening or photostiffening PEG gels with PhoCl crosslinks, termed Pho-Weak and Pho-Strong, respectively; by varying where cysteine residues were introduced with respect to the photocleavable sequence, illumination and cleavage could either cleave the protein or expose buried cysteines which could subsequently react with maleimides. However, these gels did not achieve particularly stiff elastic moduli even at the highest concentration of protein crosslinker tested ($\approx$60 Pa for Pho-Weak and $\approx$400 Pa for Pho-Strong).[193] Potentially even more excitingly, Liu et al. introduced a reversibly stiffening PEG system based on the LOV2-Jα fusion protein binding pair, which dissociates at 470 nm light, but associates in the absence of light. Using this system, the authors could pattern elastic moduli ranging from 810 to 875 Pa for studying the effects of cyclic loading on fibroblast activation.[194] More recently, Hörner et al. demonstrated optogenetic control of MSC fate and T lymphocyte migration with a fast and reversibly switchable engineered cyanobacterial phytochrome 1 (Cph1) crosslinker in a PEG matrix. The photosensory module of Cph1 with the point mutation Y263F is predominantly monomeric in far-red light ($\lambda \approx 740$ nm) and undergoes a conformational change toward the dimeric form upon exposure to red light ($\lambda \approx 660$ nm); as such, illumination with 660 nm light increased the crosslinking density of the hydrogel network, whereas illumination with 740 nm light reduced the number of crosslinks and softened the material. This was fully recoverable with subsequent cycles of light. The authors were able to achieve stiffnesses ranging from 500 to 4000 Pa based on crosslinker concentration, and saw decreases of G' by 44% upon illumination of $\lambda = 740$ nm light (Figure 6b).[195]

4.2.2. Laser-Scanning Photolithography

As with biochemical patterning, LSL provides higher resolution patterning of elastic modulus both in 2D and 3D. Focusing laser light to a specific area within a biomaterial allows photoreactions to occur near or at the focal point.[33]

Photostiffened Patterning: Single- and multiphoton LSL for photoinduced crosslinking reactions to site-specifically increase elastic modulus has been demonstrated in a variety of systems. The West group pioneered the usage of MP-LSL to pattern increased compressive modulus in PEGDA.[174] More recently, PEGDA was patterned with sinusoidal, higher molecular weight polymer strips to modify the material to display nonlinear behavior.[196] Others have showed photocaging of thiols in PEG systems with nitrobenzene or coumarin derivatives, which can be uncaged with single and multiphoton irradiation.[197,198] Additionally, pluronic-fibrinogen hydrogels that physically crosslink at 37 °C and chemically crosslink with exposure to $\lambda = 355$ nm light have been patterned with columns of stiffer and softer regions (200 and 35 Pa, respectively) to examine fibroblast morphological response to different elastic moduli.[199]

Using NIR laser beams to pattern stiffness through gold nanorod activation has become a popular method for locally increasing stiffness. Hribar et al. encapsulated gold nanorods within a PEGDA matrix, the former of which generated heat upon irradiation with a focused femtosecond NIR laser beam. This caused the network to thermally crosslink further, allowing the authors to pattern lines of different stiffnesses (17–370 kPa) (Figure 6c).[200] Stowers et al. reported on a novel alginate system with temperature-sensitive liposomes encapsulating gold nanorods and calcium, which upon heating released Ca^{2+} from the vesicle and crosslinked the surrounding alginate.[201] Chandorkar et al. recently demonstrated a similar system in poly(N-isopropylacrylamide) (pNIPAM) that exhibited mechanical actuation with frequencies up to 10 Hz when pulsed with a NIR laser and enabled dynamic studies of fibroblast actuation, cell migration changes, and nuclear translocation of MRTFA and YAP.[202]

Photosoftened Patterning: Hydrogels of PEG–acrylate (PEGA) crosslinked with PEGdiPDA have enjoyed the most use with LSL for subtractively modulating elastic modulus.[63,185] Kloxin et al. were instrumental in developing techniques with both single- and MP-LSL to pattern geometric shapes into PEGdiPDA gels to study hMSC spreading.[187] Tibbitt et al. characterized the multiphoton degradation kinetics of the system. By exploiting surface erosion at the cell–material interface, the authors could induce subcellular detachment of MSCs to better visualize and understand the effect of soft substrates on cytoskeleton rearrangement.[203] Norris et al. followed with a study demonstrating single-photon grayscale patterning of elasticity with micrometer-level resolution. MSCs congregated and aligned orthogonal to the gradient direction (**Figure 7**d).[204] Finally, coumarin-based photoactive PEG gels, which can be degraded at two-photon wavelengths between 720 and 860 nm, have shown potential in patterning crosslink density; however, this system requires a Cu catalyst, and hence, is not cytocompatible.[205]
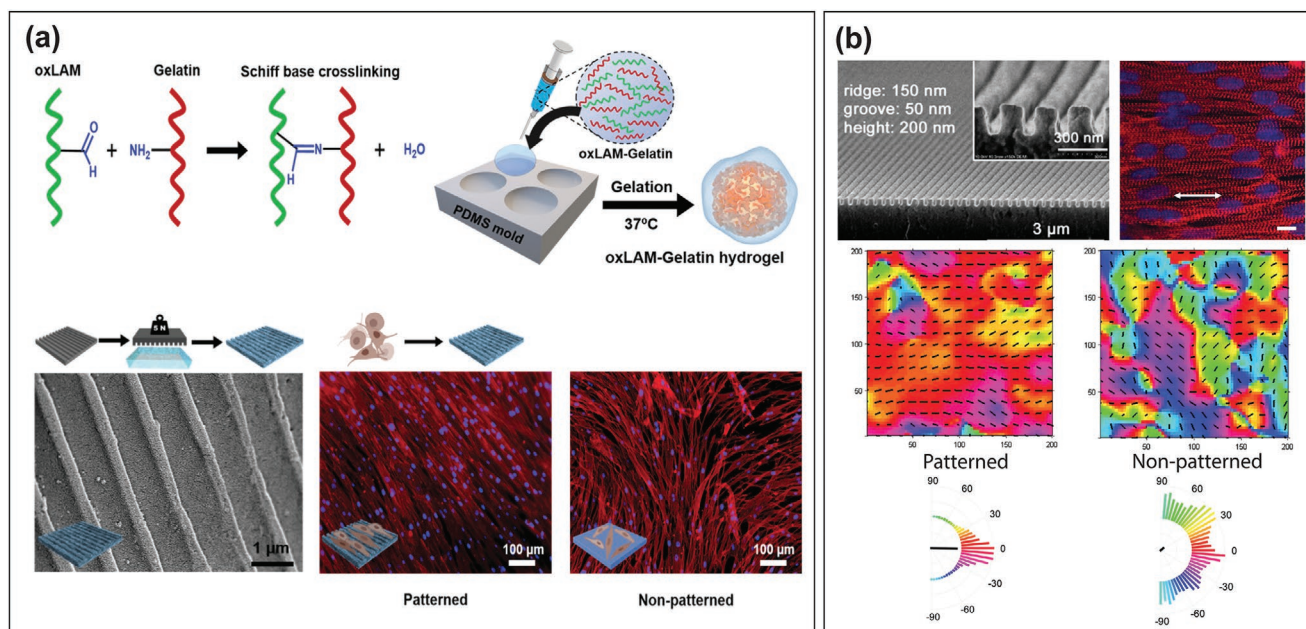
ADVANCED
Science News
www.advancedsciencenews.com

ADVANCED
MATERIALS
INTERFACES
www.advmatinterfaces.de

Figure 7. Soft lithographical patterning of topography. a) OxLAM and gelatin hydrogels can be mechanically imprinted on the micrometer scale, allowing for patterning of hASC growth. Reproduced with permission.[235] Copyright 2020, Wiley-VCH. b) Kim et al. patterned PEG on the nanoscale with CFL. Cardiomyocytes on patterned substrates grew in aligned monolayers as opposed to cells on nonpatterned substrates. Reproduced with permission.[244] Copyright 2010, National Academy of Sciences.

4.3. Soft Lithography

While soft lithographical approaches to pattern biochemical or topographical cues are common, this technique has only seen a few instances in patterning biomechanical cues; yet, it lends itself easily to patterning step changes in elasticity. The Engler group patterned PA by polymerizing the first hydrogel in a micromold, and layering a second hydrogel on top.[162,206] This method achieved 100 µm wide lines of stiffer elastic moduli (1 kPa corresponding to neurogenic; 10 kPa to myogenic; 34 kPa to osteogenic); by tailoring the elasticities, the authors induced differentiation of various cell types, creating well-defined, striated co-cultures.[206] More complex patterns have also been shown: Zhang et al. polymerized an initial PA gel in a bubble-wrap-like pattern and filled the empty space with a second hydrogel to study the effects of anisotropic stiffness gradients on invasive breast cancer cell migration. Cancer cells preferentially migrated to stiffer regions and aligned perpendicularly to the gradient, while normal cells displayed randomly oriented movement in response to anisotropy.[207]

The Lensen group utilizes a similar method, termed "fill-molding in capillaries" (FIMIC), which is commonly employed for topographical patterning; the initial prepolymer solution is patterned with a stamp, and the second prepolymer solution is then flowed into the ridges of the first hydrogel by capillary force. Diez et al. patterned alternating 20 µm wide stiff, 2.5 MPa lines with 10 µm wide soft, 240 kPa lines and observed, as expected, that fibroblasts aggregated in stiffer regions.[208] Intriguingly, a later study which performed the same method of patterning, but with a PEG and PEG–propylene(glycol) blend, observed the counterintuitive migration of fibroblasts to softer regions when the stiffer gel filled in the softer mold, avoiding

the convex, stiffer region.[209] This finding underscores the potential challenges when patterning elastic modulus using soft lithographical approaches: bi-layer gels may cause differential swelling between the two lines and cause unaccounted geometric changes in concavity and surface roughness. Additionally, as with other layering techniques, polymer depletion of the second hydrogel by the hydrogel mold may confound the prediction of layer stiffness.[162]

4.4. Additional Techniques

In addition to the methods described above, various techniques have been proposed to pattern elastic modulus. Similarly to the soft lithographical approaches discussed in Section 4.3, hydrogels have been polymerized on top of buried PDMS molds with various topographical features (e.g., balls, steps, ridges) to create gels of patterned thicknesses and stiffnesses.[210,211] Another study deployed a cunningly simple method of dehydrating and compressing ridged collagen to yield alternating, compacted lines of stiffer collagen.[212] Yang and Liang presented a method to create elastic moduli and viscoelasticity gradients in alginate gels by controlling the voltage and charge of the applied electric field.[213] E-beam lithography has also been used to pattern gelatin gels, by first inducing bond scission and radical formation and then, rearrangement and increased crosslinking in select areas.[214,215] Even more complex techniques including 3D stereolithography (SLA) have been used to create grayscale intensity patterns of PEGDMA with defined stiffnesses and geometries to study muscle cell migration.[216]

While much interest has been dedicated toward studying durotaxis and differentiation due to changes in elastic modulus, future

**ADVANCED
SCIENCE NEWS**
www.advancedsciencenews.com

**ADVANCED
MATERIALS
INTERFACES**
www.advmatinterfaces.de

work will need to incorporate other aspects of network mechanics (e.g., viscoelasticity) alongside biochemical and topographical cues to more accurately mimic the in vivo environment of the ECM.

5. Topographical Patterning of Hydrogel Substrates

In addition to biochemical and mechanical cues, the topography—the arrangement of physical features—of the ECM has proven to be instrumental in tissue differentiation and organization. In tandem with other signaling pathways, the most plausible explanations for topographical sensing is related to focal adhesion and actin fibril changes through the RhoA/ROCK pathway.[217] Early studies demonstrated that various cell types align and spread preferentially with grooved substrata in a phenomenon known as contact guidance.[218–221] Moreover, cell response varies depending on the geometric spacing and size of these cues; for instance, studies have shown that varying size of microbeads and spacing of fibronectin islands greatly affects endothelial cell proliferation.[222,223] The fate of cells can also be determined by the topographical features: for example, osteogenic differentiation of stem cells is increased in micropits.[224] Additionally, physical cues direct cell–cell coupling and orchestrate complex processes, such as myotube formation, endothelialization, and neuron projection.[225–229]

5.1. Soft Lithography

Soft lithographical approaches to patterning topographical cues are among the most popular and simple ways to explore the biological effects of topography on cells. Moreover, due to its utility and ubiquity, soft lithography has seen an expansion to other biological fields in recent years.

5.1.1. Micromolding

In one of the first instances of micromolding of hydrogels, collagen was molded with grooves of 1 µm or less to study the response of HDFB and human umbilical artery smooth muscle cells; cells aligned and proliferated in the grooves.[230] Figallo et al. expanded this to planar or tubular HA membranes which could then be laminated together to form 3D constructs.[231] Other early work patterned UV-curable, acrylate starPEG hydrogels with micro- and nanometer-scale pillars, posts, and ridges and demonstrated that fibroblasts adhere to some degree to non-biochemically functionalized surfaces with topographical patterns, depending on the spacing between the features.[232,233] Similar work in PA gels qualified the effect of gap width and shape on MSC spread area, elongation, and orientation, and found that the optimal gap width was 15 µm with surrounding heights of at least 5 µm to ensure that cells proliferated in between the features.[120] Another example in poly(2-hydroxyethyl methacrylate)-based (pHEMA) hydrogels demonstrated that arrays of micropillars of aspect ratios as high as 6 in the micrometer range promote HeLa cell adhesion on an otherwise nonadhesive surface.[234]

More recently, Lavrador et al. introduced a covalently adaptable hydrogel based on Schiff base crosslinking between oxidized laminarin, an algae-derived polysaccharide, and amine groups of gelatin. This combination of biopolymers was amenable to patterning by mechanical imprinting post gelation with micro- and nanoscale resolution. For instance, they were able to pattern the microscale ridges of a coin and a nanoarray of ridges intercalated with sub-microgrooves to align hASC growth (Figure 7a).[235]

Micromolding has expanded to more applied research, for instance, designing colonic crypt arrays, in vitro models of skeletal and cardiac muscle, and engineering microvessel structures.[236–239]

5.1.2. Capillary Force Lithography

CFL was first introduced as a technique to pattern PEGDMA substrates for biological studies in 2004 by Suh et al.[240] Stemming from this work, PEGDMA and other UV-crosslinkable PEG gels were patterned with ridges, dots, posts, and cone-shaped nanostructures. Protein adsorption and cell adhesion were greater on modified, as opposed to planar, surfaces.[241–243] Kim et al. developed a hydrogel array of nanoscale ridges and grooves as an in vitro model of the myocardium. Seeded cardiomyocytes formed aligned monolayers mimicking the native in vivo structure, as opposed to myocytes on unpatterned substrates, which were less aligned and had greater cell areas. Action potential propagation speed increased and was unidirectional on patterned substrates, unlike the elliptical propagation pattern observed on a planar gel, indicating that the underlying topography influenced cell–cell coupling and higher structural organization (Figure 7b).[244]

Agarwal et al. adapted CFL for use with alginate by taking advantage of calcium diffusion through a molded agar stamp to fabricate 15 µm wide ridges and 3 µm wide grooves in alginate films. The topography of the substrate induced anisotropy in cardiac tissue, which was able to deform the alginate substrate and generate contractile stresses comparable to healthy myocardium.[245] Nemeth et al. utilized CFL to nanopattern PEG–gelatin methacrylate (GelMA)–HA hydrogels to study chondrogenesis of dental pulp stem cells, and observed that cells formed 3D spheroids in the valleys as well as upregulated chondrogenic markers.[246] Additionally, Comelles et al. demonstrated control of topography and elastic modulus in PA gels, which promoted sustained growth of three cell lines—fibroblasts, myoblasts, and intestinal epithelial organoids—and myotube formation and differentiation.[247]

5.2. Photolithography

Photolithography has seen significant use for forming topographical patterns and more sophisticated scaffolds.

5.2.1. Mask-Based Photolithography

The early instances of masked photopatterning employed the PEGDA chemistry popularized by the West group to create

**ADVANCED
SCIENCE NEWS**

www.advancedsciencenews.com

**ADVANCED
MATERIALS
INTERFACES**

www.advmatinterfaces.de

geometric patterns on surfaces.[30,248] Generally, a base hydrogel is polymerized, and the second polymer layer on top is patterned with a mask to yield topographical reliefs in a bottom-up approach.[30] Bryant and Ratner introduced photosensitive pHEMA with tunable polymerization kinetics based on light exposure: the covered areas experienced no inhibition of polymerization, whereas in the exposed regions the polymerization and photodegradation of the crosslinker were in competition, yielding partially or non-crosslinked areas, depending on the intensity of the light transmitted.[249,250] However, both of these techniques do not yield high precision patterning, as features below 200 µm are difficult to achieve.[30,250]

As such, photodegradable chemistries have been explored for top-down approaches to patterning. Fairbanks et al. reported a novel mechanism for photochemically cleaving disulfide crosslinked hydrogels, which could also be mechanically imprinted due to the reversible nature of the bonds.[251] Patterning schemes based on the photodegradable oNB chemistry have also been demonstrated, stemming from the work done by Kloxin et al. which used photomasks to erode channels to control hMSC spreading.[90,187] Further studies incorporated the degradable acrylate chemistry such as the dual-tone system presented by Xue et al. and the geometric patterning done by Kirschner et al., which demonstrated that hMSCS elongated and spread in proportion to the aspect ratio of the patterned topographical features.[252,253] Nikkhah et al. explored patterning GelMA with a photomask to generate ridges of 50 µm wide with heights ranging from 50 to 150 µm and showed that HUVECs aligned along the major axis and formed endothelial cord structures.[254]

5.2.2. Laser-Scanning Lithography

Higher precision and 3D patterning of substrates with LSL as opposed to masked photolithography has spurred many developments in photosensitive chemistries. While some work has been performed using single-photon-based patterning to study hMSC spreading and orientation,[187,253] and neuron outgrowth,[255] most studies have employed multiphoton techniques for both photoadditive and photoablative chemistries. For instance, Qin et al. modified gelatin hydrolysate with vinyl esters, enabling them to selectively crosslink 500 µm hexagonal rings that could be fused together for more complex scaffolds.[256] Collagen hydrogels with embedded gold nanorods have also been used for patterning channels to guide endothelial cell migration, alignment, and tube formation.[257] In a similar manner, microstructures of concentric squares or lines with sub-micrometer resolution were selectively crosslinked on MeHA gels, and modified with a laminin-derived peptide (IKVAV) to direct Schwann and neuronal cell growth in 2D and 3D.[258] Hippler et al. introduced secondary patterning of 3D printed pNIPAM crosslinked with photosensitive N,N´-methylenebisacrylamide; upon irradiation with a NIR laser, local heating and stiffening occurred, bending posts in the desired direction.[259]

On the other hand, photodegradable chemistries represent another approach to making topographical patterns. As with chemical and mechanical patterning, the oNB group has

commonly been employed as a photolabile moiety. In their seminal work, Kloxin et al. deployed photocleavable PEG–diPDA to degrade interconnected 3D channels in a gel, releasing fibrosarcoma cells into the channel and enabling migration.[63] Following this, Kloxin et al. also installed this functional group in a di-azide enzymatically cleavable crosslinker for reaction with PEG–tetracyclooctyne. Using two-photon lithography, wells were photodegraded and seeded with AT2 cells; subsequently, the wells were filled in with gel precursor, but the geometry and interconnectivity of the wells could be changed on demand.[260] A photodegradable step-growth network containing the oNB linker and formed through SPAAC has been utilized to govern 3D endothelial cell outgrowth with PEG-based hydrogels, a strategy recently extended to guide axonal growth.[90,261] Arakawa et al. eroded 3D vascular beds by installing a photodegradable oNB group into a diazide peptide crosslinker.[262] To further increase sensitivity, coumarin groups have been coupled with oNB groups or directly attached to the PEG macromer.[205,263]

Others have turned to material photoablation for topographical patterning, whereby high-power lasers indiscriminately sever covalent linkages comprising the gel backbone. Brandenberg and Lutolf patterned microvasculature networks in various natural hydrogels, which could then be perfused.[264] Arakawa et al. also employed a similar approach in collagen hydrogels to create a fully perfusable capillary model.[265] A recent composite approach incorporated graphene oxide into PA, rendering it sensitive to femtosecond laser ablation, for patterning lines between 20 and 80 µm wide. 50 µm wide lines were found to be the most successful at facilitating differentiation and alignment. Furthermore, the chemical reduction of the graphene oxide resulted in improved electrical conductance and efficient delivery of external electrical signals to the myoblasts.[227]

5.3. Electrospinning

Electrospinning provides a simple and versatile method for creating fibers, mimicking the fibrous nature of the ECM. A high voltage is applied to a polymer solution to induce a liquid jet, which is then continuously stretched due to the electrostatic repulsions between the surface charges and the evaporation of the solvent.[266] The arrangement, shape, and movement of the collector plate can determine the deposition and size of the fibers, permitting creation of highly aligned fibers to study cell response. To accomplish this type of patterning, rotating drums or other specially designed collectors are generally utilized.

In one of the first studies utilizing hydrogel polymeric precursors, Kakade et al. produced aligned PEG fibers on both the macroscopic and polymeric level by collecting on electrically counter-charged plates.[267] Liu et al. electrospun micrometer-thick PEG poly(DL-lactide) fibers on a lithographically patterned conductive collector to make ridges and valleys. NIH 3T3 cells preferentially migrated and invaded the ridges, and deposited ECM in alignment with the fibers.[268] As a more high-throughput approach to generating aligned fibers, Hou et al. developed a dynamic crosslinking method to make size-controllable, isotropically swelling fibers from PEGDA in a large bath with an adjacent fiber collection roller to capture the fibers.[269]

**ADVANCED
SCIENCE NEWS**
www.advancedsciencenews.com

**ADVANCED
MATERIALS
INTERFACES**
www.advmatinterfaces.de

Multiple studies have compared the difference between random and aligned fibers on cell mechanotransduction. Nivison-Smith and Weiss compared the effect of isotropic and random fibers from recombinant human tropoelastin on the alignment of primary coronary artery SMCs and demonstrated that SMCs on aligned scaffolds form an elongated and directional monolayer.[270] PCL–gelatin fibers were used to compare fibroblast alignment and gene expression on aligned and random mats: eight genes connected to focal adhesion formation and actin polymerization were upregulated.[271] Furthermore, Yao et al. demonstrated that soft, hierarchically aligned fibrillar, as opposed to random fibrin hydrogels promoted neurogenic differentiation of MSCs and induced neurite outgrowths up to 2 mm long.[272]

There has also been work with incorporating and patterning electrospun micro or nanofibers into hydrogels. Aligned PLLA nanofibers were microcontact printed on agarose.[273] Additionally, PCL fibers were embedded in PEGDA, and then patterned with a photomask to create ridges of aligned, perpendicular, and random fibers. Myoblast differentiation was affected by the direction of nanofibers, more so than the micropatterns of the gels.[274] Song et al. designed an intricate method for making layered hydrogels: they created patterned topographical collectors by soft lithography, and electrospun nylon fibers to create mats with posts. These mats were transferred to a Matrigel hydrogel, and seeded with human embryonic stem cells; these cells were allowed to adhere and filled in with alginate, creating a confluent interface of two hydrogel materials.[275] Electrospinning has been a critical technique in exploring alignment in matrices similar to the native ECM and has begun to elucidate critical roles for fibers in the cell's environment.

5.4. 3D Printing

3D printing has revolutionized 3D tissue culture and has been instrumental in developing larger, multicellular constructs. Herein, we present a select few instances to design topographical arrays to study cellular response; we note, however, that many other review articles discuss this technology and its potential applications in greater depth.[276,277]

5.4.1. Light-Based 3D Printing

SLA utilizes light to sculpt objects from photocurable resins (e.g., hydrogel precursors). A laser is rastered over a liquid resin, polymerizing a volume unit (a "voxel") of polymer, and is repeated layer by layer until completion.[276] While this type of additive manufacturing was developed in the 1980s, its use with hydrogel materials began to be explored in the early 2000s. Itoga et al. micropatterned convex PEGDA domains on glass slides, and achieved cell adhesion in absence biochemical cues to the dome patterns.[278] Valentin et al. described an exciting and novel method for SLA printing alginate: photoacid generators were selectively illuminated in the presence of insoluble cation salts, which would dissolve in the presence of H+ ions and crosslink alginate strands. They could pattern ridges of different heights, steps and microfluidic channels with tall

reservoirs. The reservoirs could be degraded with a chelator to release cells and study collective cell migration. The authors observed that monolayers with an initially convex geometry were pulled forward faster than flat geometries due to supramolecular actomyosin cables (**Figure 8**a).[279]

Newer and faster methods, such as digital projection lithography (DLP), continuous liquid interface production (CLIP), and two-photon polymerization (2PP) are based on the same concept, but in contrast to standard SLA, use micromirror devices or dynamic liquid crystal masks to project the desired image and as such, enable polymerization of an entire layer.[276] Various reports have demonstrated the utility of DLP in designing biocompatible PEGDA scaffolds with controlled geometries, pore size, and crosslinking densities, leading to swelling-induced patterns.[280–282] Naturally derived materials have also been employed for DLP. Gauvin et al. printed controlled, porous GelMA scaffolds in microscale hexagonal and log cabin patterns to allow for uniform cell distribution, and Soman et al. demonstrated intricate geometric patterns such as flowers, spirals and pyramids in GelMA that cells could deform and move.[283,284] Ma et al. 3D bioprinted a hexagonal GelMA lattice seeded with hIPSCs and HUVECs or ADSCs in defined locations as a patient-specific hepatic model; cells preferentially aligned where they were seeded and upregulated production of key enzymes related to drug metabolism (Figure 8b).[285]

For more precise control over architecture, Yin et al. reported on an oxygen inhibition-assisted CLIP technique that enabled design of environments in PEGDMA with defined geometries and stiffnesses.[216] As an example of the most advanced and highest resolution technique, Klein et al. manufactured PEGDA/pentaerythritol tetracrylate copolymer micropillars with interconnecting beams, and tethered photoresist cubes with deposited ECM molecules to the beams using 2PP. The precise placement of the cubes bestowed control of singular fibroblast adhesion, shape, and orientation in 3D space, offering an exciting platform for future studies of spatial ligand and topographical cue presentation.[286]

5.4.2. Ink-Based 3D Printing

While light-based 3D printing provides the highest resolution, it is limited to photopolymerizable materials; on the other hand, ink-based 3D printing can be applied to a variety of soft materials. Direct-write printing is a method whereby a syringe with a nozzle is moved over a surface as it dispenses ink. Through careful control of ink composition, printing parameters, and rheological behavior, 3D constructs, such as high aspect ratio walls, continuous solids or spanning features can be constructed.[287] Barry et al. direct wrote a mixture of acrylamide and glycerol to make hydrogel scaffolds with 5 μm thick filaments with 20 μm spacing and noted that fibroblasts tended to grow down into the well, at the bottom of the ridges.[288] Others have proposed utilizing the pluronic family of polymers, due to their shear-thinning properties, temperature sensitivity, biocompatibility, and potential to be chemically modified with acrylate groups for permanent crosslinking.[289,290] For example, the Lewis group presented an elegant strategy printing a patterned microvasculature system: fugitive pluronic filaments
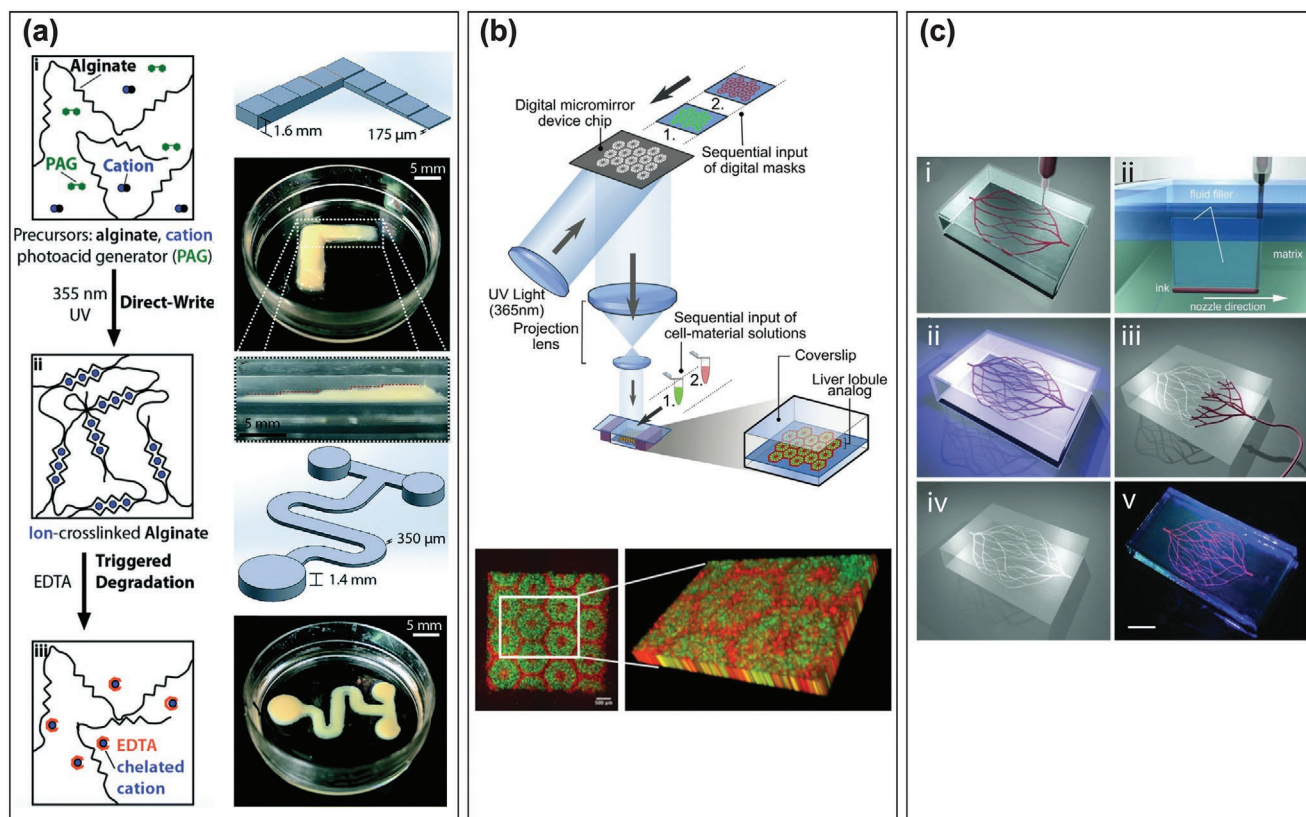
**ADVANCED
SCIENCE NEWS**

www.advancedsciencenews.com

**ADVANCED
MATERIALS
INTERFACES**

www.advmatinterfaces.de

Figure 8. 3D Printing techniques for patterning topography. a) Alginate with cation photoacid generators (left) was stereolithographically 3D printed in multiple unique designs (right). Reproduced with permission.[279] Copyright 2017, Royal Society of Chemistry. b) Ma et al. printed a patient-specific hexagonal GelMA lattices using DLP to model the liver. Reproduced with permission.[285] Copyright 2016, National Academy of Sciences. c) The Lewis group's method to omnidirectionally print vascular structures with fugitive pluronic ink. Reproduced with permission.[291] Copyright 2011, Wiley-VCH.

were extruded into a photocurable reservoir of F127-diacrylate and after matrix polymerization, were washed out, yielding defined void structures (Figure 8c).[291] PEG-based systems have seen limited use, but some examples of copolymers exist in the literature. Dual stimuli-responsive diblock and triblock copolymers based on poly(alkyl glycidyl ether), poly(isopropyl glycidyl ether), and PEG have been used to direct write microscale free-standing pillars with aspect ratios of up to 23.[292]

5.5. Additional Techniques

Other techniques for patterning topographies such as e-beam lithography, nanoimprint lithography (NIL), and microfluidic approaches have been suggested.[293,294] Particularly interesting examples are discussed below. A hybrid poly(acrylic acid) (PAA) and bacteriorhodopsin (BR) gel was crosslinked with e-beam lithography; at low pH conditions, the carboxyl groups of PAA dissociated, leading to osmotic pressure buildup and significant chain stretching. Exposing the gel to green light induced conformational change in BR, resulting in a flux of protons, protonation of PAA and a return to the original state.[295] Dos Reis et al. also utilized e-beam lithography to etch networks of microwells and channels in acryloyl end-capped hydrogels to promote neurite extension.[296] NIL—a hard lithographical

molding technique that generates resist relief patterns on the nanometer scale by physically compressing the imprint resist as it is curing—was used to pattern gratings and pillars in poly(vinyl alcohol) planar and tubular vascular grafts.[297] The topographical patterns encouraged endothelialization and patency in vivo after 20 days, leading the authors to propose that the hydrophobicity of the surface is impacted by the nanoscale topographies and may allow for cells to adhere without surface modifications.[298] Additionally, PA gels with embedded nickel microwires which were aligned with magnets to create wrinkled surfaces were used to study VSMC response to dynamic changes in topography.[299]

Surface wrinkling of hydrogels caused by differences in osmotic pressure has seen a surge in interest for patterning applications.[300,301] The Hayward group has demonstrated control over buckling patterns by changing gel thickness, crosslinking density, UV and air exposure, and layering multiple gels, enabling them to create hexagonal, lamellar, and conical patterns, among others.[302–304] Hughes et al. demonstrated that wrinkled PEGDA microposts could be produced by balancing competing polymerization and termination events due to oxygen inhibition. Using this platform, they showed that fibroblasts migrated out of wells and attached to wrinkled posts, assuming a 3D morphology and even coupled with other cells nearby.[225] In the future, with a better understanding of surface

wrinkling properties, the exploitation of this physical phenomenon may present a simpler way to generate smaller-scale patterns for use in tissue engineering or cell culture applications.

6. Conclusion

The field of hydrogel patterning has seen significant advancement in the past two decades, enabling researchers to probe cellular interactions in vitro and engineer elegant multicellular structures, yet there is always room for innovation, both in materials and techniques. In particular, future work should focus on designing more cytocompatible chemistries, engineering true reversibility of cue presentation, boosting patterning resolution while not sacrificing precision, and modifying and expanding upon current techniques to extend patterning to 3D and other materials. To achieve these goals, we must integrate advances from both chemical and technological perspectives.

Recent advances in material chemistry and protein engineering have shown compounds or proteins that are dual-wavelength sensitive, such as those based on *cis–trans* azobenzene isomerization, guest–host interactions of azobenzene and *β*-cyclodextrin, photoreceptors such as Dronpa145N, and split-protein systems.[305–310] Such control would allow studies of spatial and temporal presentation of biochemical and mechanical cues previously inaccessible, without having to transfer cells to other substrates, and provide a route to more accurately model the ever-changing niche that cells encounter in vivo. Additionally, combining orthogonal or multiplexed materials is another route to patterning multiple gel aspects, potentially enabling users to pattern biochemical, mechanical, and topographical cues in one system. Advances in supramolecular chemistry may further expand physiochemical control over hydrogel constructs.

Combining improvements in material development with technological advances may not only provide increased patterning resolution but also an opportunity for scaling up fabrication processes. However, it is challenging to select the right material and technique to ensure optimal resolution and biocompatibility. For example, although advances in photolithography, specifically in using multiphoton lasers, have addressed cytotoxicity concerns while still providing excellent resolution, the slower processing speed of MP-LSL limits its application in scaling up for high-throughput studies and larger fabrication volumes. Furthermore, with scan-based patterning, simultaneous targeting of multiple sites within a given area is not possible and is limited by the sequential laser scanning process. Recently, emerging tools in the optics community have been proposed to address these challenges. Parallel stimulation can be achieved by spatial light modulators (SLM), which allow for the controlled projection of light patterns either by manipulating the intensity (amplitude) or phase of the light. Digital mirror devices, amplitude SLM made up of thousands to millions of microscopic mirrors that are capable of being independently turned "on" or "off," have been used to control spatiotemporal light patterns with resolution on the micrometer scale without the need for a mask.[311] Holographic illumination, a phase SLM where computer-generated phase holograms are used to make patterns, provides additional advantages, including high efficiency and its ability to produce 3D light patterns.[312] Although SLM allows for dynamic pattern changes, the resolution is limited by the mirror number, shape, and density.[313] Furthermore, the writing speed is limited by the laser power. Technological advances in high pulse power kHz repetition lasers have enabled massive parallelization of interface patterning. These high-power lasers can be combined with SLM or fixed diffractive optical elements (DOE) to fabricate repetitive periodic patterns. Parallelization can be achieved through DOE, which can be inserted into the beam path to create multiple beamlets.[313] Fabrication speed can also be increased through resonant-scanning-based lithography.[314]

Together, these techniques and advances in fabrication and material chemistry provide greater control over directing cell fate by allowing simultaneous and independent stimulation of cells with biochemical, mechanical, and topographical cues. Overall, platforms that can spatially and temporally present biochemical and biophysical cues will become integral in exploring novel regenerative medicine approaches and studying new pathways of disease in more realistic models.

Conflict of Interest

The authors declare no conflict of interest.

[1] E. Ruoslahti, M. D. Pierschbacher, *Science* **1987**, *238*, 491.
[2] C. F. Guimarães, L. Gasperini, A. P. Marques, R. L. Reis, *Nat. Rev. Mater.* **2020**, *5*, 351.
[3] C. M. Madl, S. C. Heilshorn, *Annu. Rev. Biomed. Eng.* **2018**, *20*, 21.
[4] M. G. Rubashkin, G. Ou, V. M. Weaver, *Biochemistry* **2014**, *53*, 2078.
[5] J. R. Tse, A. J. Engler, *PLoS One* **2011**, *6*, 15978.
[6] K. R. Levental, H. Yu, L. Kass, J. N. Lakins, M. Egeblad, J. T. Erler, S. F. T. Fong, K. Csiszar, A. Giaccia, W. Weninger, M. Yamauchi, D. L. Gasser, V. M. Weaver, *Cell* **2009**, *139*, 891.
[7] P. Martin, *Science* **1997**, *276*, 75.
[8] T. E. Brown, K. S. Anseth, *Chem. Soc. Rev.* **2017**, *46*, 6532.
[9] A. S. Hoffman, *Adv. Drug Delivery Rev.* **2012**, *64*, 18.

**ADVANCED
SCIENCE NEWS**

www.advancedsciencenews.com

**ADVANCED
MATERIALS
INTERFACES**

www.advmatinterfaces.de

[10] T. E. Brown, K. S. Anseth, *Chem. Soc. Rev.* **2017**, *46*, 6532.

[11] S. Turunen, A. M. Haaparanta, R. Äänismaa, M. Kellomäki, *J. Tissue Eng. Regener. Med.* **2013**, *7*, 253.

[12] K. T. M. Tran, T. D. Nguyen, *J. Sci. Adv. Mater. Devices* **2017**, *2*, 1.

[13] M. Altissimo, *Biomicrofluidics* **2010**, *4*, 026503.

[14] G. M. Whitesides, E. Ostuni, S. Takayama, X. Jiang, D. E. Ingber, *Annu. Rev. Biomed. Eng.* **2001**, *3*, 335.

[15] Y. Xia, G. M. Whitesides, *Angew. Chem., Int. Ed.* **1998**, *37*, 550.

[16] J. M. Huffman, J. Shao, C. H. Hsu, A. Folch, *Adv. Mater.* **2004**, *16*, 2201.

[17] A. G. Castaño, V. Hortigüela, A. Lagunas, C. Cortina, N. Montserrat, J. Samitier, E. Martínez, *RSC Adv.* **2014**, *4*, 29120.

[18] K. Y. Suh, H. H. Lee, *Adv. Funct. Mater.* **2002**, *12*, 405.

[19] H. Li, C. Tan, L. Li, *Mater. Des.* **2018**, *159*, 20.

[20] S. Ilkhanizadeh, A. I. Teixeira, O. Hermanson, *Biomaterials* **2007**, *28*, 3936.

[21] R. D. Pedde, B. Mirani, A. Navaei, T. Styan, S. Wong, M. Mehrali, A. Thakur, N. K. Mohtaram, A. Bayati, A. Dolatshahi-Pirouz, M. Nikkhah, S. M. Willerth, M. Akbari, *Adv. Mater.* **2017**, *29*, 1606061.

[22] J. P. Renault, A. Bernard, A. Bietsch, B. Michel, H. R. Bosshard, E. Delamarche, M. Kreiter, B. Hecht, U. P. Wild, *J. Phys. Chem. B* **2003**, *107*, 703.

[23] L. Pardo, W. Cris Wilson, T. Boland, *Langmuir* **2003**, *19*, 1462.

[24] D. L. Hern, J. A. Hubbell, *J. Biomed. Mater. Res.* **1998**, *39*, 266.

[25] J. B. Leach, K. A. Bivens, C. N. Collins, C. E. Schmidt, *J. Biomed. Mater. Res., Part A* **2004**, *70A*, 74.

[26] K. Ghosh, X. D. Ren, X. Z. Shu, G. D. Prestwich, R. A. F. Clark, *Tissue Eng.* **2006**, *12*, 601.

[27] C. C. Lin, P. D. Boyer, A. A. Aimetti, K. S. Anseth, *J. Controlled Release* **2010**, *142*, 384.

[28] J. D. McCall, J. E. Luoma, K. S. Anseth, *Drug Delivery Transl. Res.* **2012**, *2*, 305.

[29] M. B. Browning, B. Russell, J. Rivera, M. Höök, E. M. Cosgriff-Hernandez, *Biomacromolecules* **2013**, *14*, 2225.

[30] M. S. Hahn, L. J. Taite, J. J. Moon, M. C. Rowland, K. A. Ruffino, J. L. West, *Biomaterials* **2006**, *27*, 2519.

[31] J. J. Moon, M. S. Hahn, I. Kim, B. A. Nsiah, J. L. West, *Tissue Eng., Part A* **2009**, *15*, 579.

[32] T. T. Lee, J. R. García, J. I. Paez, A. Singh, E. A. Phelps, S. Weis, Z. Shafiq, A. Shekaran, A. Del Campo, A. J. García, *Nat. Mater.* **2015**, *14*, 352.

[33] E. R. Ruskowitz, C. A. DeForest, *Nat. Rev. Mater.* **2018**, *3*, 17087.

[34] J. Gopinathan, I. Noh, *Tissue Eng. Regener. Med.* **2018**, *15*, 531.

[35] B. D. Polizzotti, B. D. Fairbanks, K. S. Anseth, *Biomacromolecules* **2008**, *9*, 1084.

[36] B. J. Adzima, Y. Tao, C. J. Kloxin, C. A. DeForest, K. S. Anseth, C. N. Bowman, *Nat. Chem.* **2011**, *3*, 256.

[37] C. A. DeForest, B. D. Polizzotti, K. S. Anseth, *Nat. Mater.* **2009**, *8*, 659.

[38] C. A. DeForest, E. A. Sims, K. S. Anseth, *Chem. Mater.* **2010**, *22*, 4783.

[39] F. Yu, X. Cao, Y. Li, X. Chen, *ACS Macro Lett.* **2015**, *4*, 289.

[40] B. D. Fairbanks, M. P. Schwartz, A. E. Halevi, C. R. Nuttelman, C. N. Bowman, K. S. Anseth, *Adv. Mater.* **2009**, *21*, 5005.

[41] L. A. Sawicki, A. M. Kloxin, *Biomater. Sci.* **2014**, *2*, 1612.

[42] W. M. Gramlich, I. L. Kim, J. A. Burdick, *Biomaterials* **2013**, *34*, 9803.

[43] T. B. Dorsey, A. Grath, A. Wang, C. Xu, Y. Hong, G. Dai, *Bioact. Mater.* **2018**, *3*, 64.

[44] X. Tong, J. Jiang, D. Zhu, F. Yang, *ACS Biomater. Sci. Eng.* **2016**, *2*, 845.

[45] L. A. Sawicki, A. M. Kloxin, *J. Visualized Exp.* **2016**, *2016*, 54462.

[46] R. J. Wade, E. J. Bassin, W. M. Gramlich, J. A. Burdick, *Adv. Mater.* **2015**, *27*, 1356.

[47] D. L. Alge, M. A. Azagarsamy, D. F. Donohue, K. S. Anseth, *Biomacromolecules* **2013**, *14*, 949.

[48] S. L. Vega, M. Y. Kwon, K. H. Song, C. Wang, R. L. Mauck, L. Han, J. A. Burdick, *Nat. Commun.* **2018**, *9*, 614.

[49] I. S. Carrico, S. A. Maskarinec, S. C. Heilshorn, M. L. Mock, J. C. Liu, P. J. Nowatzki, C. Franck, G. Ravichandran, D. A. Tirrell, *J. Am. Chem. Soc.* **2007**, *129*, 4874.

[50] W. Lee, D. Choi, Y. Lee, D. N. Kim, J. Park, W. G. Koh, *Sens. Actuators, B* **2008**, *129*, 841.

[51] B. Joddar, A. T. Guy, H. Kamiguchi, Y. Ito, *Biomaterials* **2013**, *34*, 9593.

[52] P. Bhatnagar, G. G. Malliaras, I. Kim, C. A. Batt, *Adv. Mater.* **2010**, *22*, 1242.

[53] C. A. DeForest, D. A. Tirrell, *Nat. Mater.* **2015**, *14*, 523.

[54] J. A. Shadish, G. M. Benuska, C. A. DeForest, *Nat. Mater.* **2019**, *18*, 1005.

[55] P. E. Farahani, S. M. Adelmund, J. A. Shadish, C. A. DeForest, *J. Mater. Chem. B* **2017**, *5*, 4435.

[56] Y. Dong, G. Jin, Y. Hong, H. Zhu, T. J. Lu, F. Xu, D. Bai, M. Lin, *ACS Appl. Mater. Interfaces* **2018**, *10*, 12374.

[57] M. Kamimura, M. Sugawara, S. Yamamoto, K. Yamaguchi, J. Nakanishi, *Biomater. Sci.* **2016**, *4*, 933.

[58] S. Yamamoto, K. Okada, N. Sasaki, A. C. Chang, K. Yamaguchi, J. Nakanishi, *Langmuir* **2019**, *35*, 7459.

[59] Y. Shi, V. X. Truong, K. Kulkarni, Y. Qu, G. P. Simon, R. L. Boyd, P. Perlmutter, T. Lithgow, J. S. Forsythe, *J. Mater. Chem. B* **2015**, *3*, 8771.

[60] C. T. Huynh, M. K. Nguyen, G. Y. Tonga, L. Longé, V. M. Rotello, E. Alsberg, *Adv. Healthcare Mater.* **2016**, *5*, 305.

[61] D. R. Griffin, A. M. Kasko, *ACS Macro Lett.* **2012**, *1*, 1330.

[62] P. J. LeValley, R. Neelarapu, B. P. Sutherland, S. Dasgupta, C. J. Kloxin, A. M. Kloxin, *J. Am. Chem. Soc.* **2020**, *142*, 4671.

[63] A. M. Kloxin, A. M. Kasko, C. N. Salinas, K. S. Anseth, *Science* **2009**, *324*, 59.

[64] P. M. Gawade, J. A. Shadish, B. A. Badeau, C. A. DeForest, *Adv. Mater.* **2019**, *31*, 1902462.

[65] J. A. Shadish, A. C. Strange, C. A. DeForest, *J. Am. Chem. Soc.* **2019**, *141*, 15619.

[66] Z. Zhang, J. Du, Y. Li, J. Wu, F. Yu, Y. Chen, *J. Mater. Chem. B* **2017**, *5*, 5974.

[67] Z. Zhang, C. Liu, C. Yang, Y. Wu, F. Yu, Y. Chen, J. Du, *ACS Appl. Mater. Interfaces* **2018**, *10*, 8546.

[68] C. A. DeForest, K. S. Anseth, *Angew. Chem., Int. Ed.* **2012**, *51*, 1816.

[69] N. R. Gandavarapu, M. A. Azagarsamy, K. S. Anseth, *Adv. Mater.* **2014**, *26*, 2521.

[70] J. C. Grim, T. E. Brown, B. A. Aguado, D. A. Chapnick, A. L. Viert, X. Liu, K. S. Anseth, *ACS Cent. Sci.* **2018**, *4*, 909.

[71] N. Wang, Y. Li, Y. Zhang, Y. Liao, W. Liu, *Langmuir* **2014**, *30*, 11823.

[72] J. A. Shadish, C. A. DeForest, *Matter* **2020**, *2*, 50.

[73] J. A. Hammer, A. Ruta, J. L. West, *Ann. Biomed. Eng.* **2020**, *48*, 1885.

[74] M. S. Hahn, J. S. Miller, J. L. West, *Adv. Mater.* **2005**, *17*, 2939.

[75] M. S. Hahn, J. S. Miller, J. L. West, *Adv. Mater.* **2006**, *18*, 2679.

[76] J. E. Leslie-Barbick, C. Shen, C. Chen, J. L. West, *Tissue Eng., Part A* **2011**, *17*, 221.

[77] S. H. Lee, J. J. Moon, J. L. West, *Biomaterials* **2008**, *29*, 2962.

[78] J. C. Hoffmann, J. L. West, *Soft Matter* **2010**, *6*, 5056.

[79] J. C. Culver, J. C. Hoffmann, R. A. Poché, J. H. Slater, J. L. West, M. E. Dickinson, *Adv. Mater.* **2012**, *24*, 2344.

[80] Y. Luo, M. S. Shoichet, *Nat. Mater.* **2004**, *3*, 249.

[81] J. H. Wosnick, M. S. Shoichet, *Chem. Mater.* **2008**, *20*, 55.

[82] Y. Aizawa, R. Wylie, M. Shoichet, *Adv. Mater.* **2010**, *22*, 4831.

[83] R. G. Wylie, S. Ahsan, Y. Aizawa, K. L. Maxwell, C. M. Morshead, M. S. Shoichet, *Nat. Mater.* **2011**, *10*, 799.

[84] Y. Aizawa, M. S. Shoichet, *Biomaterials* **2012**, *33*, 5198.

**ADVANCED
SCIENCE NEWS**

www.advancedsciencenews.com

**ADVANCED
MATERIALS
INTERFACES**

www.advmatinterfaces.de

[85] S. C. Owen, S. A. Fisher, R. Y. Tam, C. M. Nimmo, M. S. Shoichet, *Langmuir* **2013**, *29*, 7393.

[86] S. A. Fisher, R. Y. Tam, A. Fokina, M. M. Mahmoodi, M. D. Distefano, M. S. Shoichet, *Biomaterials* **2018**, *178*, 751.

[87] K. A. Mosiewicz, L. Kolb, A. J. Van Der Vlies, M. M. Martino, P. S. Lienemann, J. A. Hubbell, M. Ehrbar, M. P. Lutolf, *Nat. Mater.* **2013**, *12*, 1072.

[88] V. X. Truong, F. Li, J. S. Forsythe, *Biomacromolecules* **2018**, *19*, 4277.

[89] N. Labòria, R. Wieneke, R. Tampé, *Angew. Chem., Int. Ed.* **2013**, *52*, 848.

[90] C. A. DeForest, K. S. Anseth, *Nat. Chem.* **2011**, *3*, 925.

[91] N. Broguiere, I. Lüchtefeld, L. Trachsel, D. Mazunin, R. Rizzo, J. W. Bode, M. P. Lutolf, M. Zenobi-Wong, *Adv. Mater.* **2020**, *32*, 1908299.

[92] S. K. Seidlits, C. E. Schmidt, J. B. Shear, *Adv. Funct. Mater.* **2009**, *19*, 3543.

[93] A. D. Rape, M. Zibinsky, N. Murthy, S. Kumar, *Nat. Commun.* **2015**, *6*, 8129.

[94] Y. Zheng, M. K. Liong Han, Q. Jiang, B. Li, J. Feng, A. Del Campo, *Mater. Horiz.* **2020**, *7*, 111.

[95] P. J. Dorsey, M. Rubanov, W. Wang, R. Schulman, *ACS Macro Lett.* **2019**, *8*, 1133.

[96] T. Kaufmann, B. J. Ravoo, *Polym. Chem.* **2010**, *1*, 371.

[97] M. R. Burnham, J. N. Turner, D. Szarowski, D. L. Martin, *Biomaterials* **2006**, *27*, 5883.

[98] M. R. Hynd, J. P. Frampton, N. Dowell-Mesfin, J. N. Turner, W. Shain, *J. Neurosci. Methods* **2007**, *162*, 255.

[99] M. R. Hynd, J. P. Frampton, M. R. Burnham, D. L. Martin, N. M. Dowell-Mesfin, J. N. Turner, W. Shain, *J. Biomed. Mater. Res., Part A* **2007**, *81A*, 347.

[100] T. Grevesse, M. Versaevel, G. Circelli, S. Desprez, S. Gabriele, *Lab Chip* **2013**, *13*, 777.

[101] J. Lee, A. A. Abdeen, D. Zhang, K. A. Kilian, *Biomaterials* **2013**, *34*, 8140.

[102] Y. Bin Lee, S.-J. Kim, E. M. Kim, H. Byun, H. kwan Chang, J. Park, Y. S. Choi, H. Shin, *Acta Biomater.* **2017**, *61*, 75.

[103] F. Ren, C. Yesildag, Z. Zhang, M. C. Lensen, *Chem. Mater.* **2017**, *29*, 2008.

[104] C. Yesildag, Z. Ouyang, Z. Zhang, M. C. Lensen, *Front. Chem.* **2019**, *6*, 667.

[105] H. Yu, S. Xiong, C. Y. Tay, W. S. Leong, L. P. Tan, *Acta Biomater.* **2012**, *8*, 1267.

[106] F. Di Benedetto, A. Biasco, D. Pisignano, R. Cingolani, *Nanotechnology* **2005**, *16*, S165.

[107] I. Sanzari, M. Callisti, A. De Grazia, D. J. Evans, T. Polcar, T. Prodromakis, *Sci. Rep.* **2017**, *7*, 5764.

[108] I. Sanzari, E. J. Humphrey, F. Dinelli, C. M. Terracciano, T. Prodromakis, *Sci. Rep.* **2018**, *8*, 11991.

[109] X. Tang, M. Yakut Ali, M. T. A. Saif, *Soft Matter* **2012**, *8*, 7197.

[110] K. L. Christman, E. Schopf, R. M. Broyer, R. C. Li, Y. Chen, H. D. Maynard, *J. Am. Chem. Soc.* **2009**, *131*, 521.

[111] R. M. Broyer, E. Schopf, C. M. Kolodziej, Y. Chen, H. D. Maynard, *Soft Matter* **2011**, *7*, 9972.

[112] R. J. Mancini, S. J. Paluck, E. Bat, H. D. Maynard, *Langmuir* **2016**, *32*, 4043.

[113] W. C. Wilson, T. Boland, *Anat. Rec., Part A* **2003**, *272A*, 491.

[114] T. Boland, V. Mironov, A. Gutowska, E. A. Roth, R. R. Markwald, *Anat. Rec., Part A* **2003**, *272A*, 497.

[115] T. Boland, T. Xu, B. Damon, X. Cui, *Biotechnol. J.* **2006**, *1*, 910.

[116] T. Xu, J. Jin, C. Gregory, J. J. Hickman, T. Boland, *Biomaterials* **2005**, *26*, 93.

[117] U. A. Gurkan, R. El Assal, S. E. Yildiz, Y. Sung, A. J. Trachtenberg, W. P. Kuo, U. Demirci, *Mol. Pharmaceutics* **2014**, *11*, 2151.

[118] R. Mateen, M. M. Ali, T. Hoare, *Nat. Commun.* **2018**, *9*, 602.

[119] N. E. Fedorovich, J. R. De Wijn, A. J. Verbout, J. Alblas, W. J. A. Dhert, *Tissue Eng., Part A.* **2008**, *14*, 127.

[120] M. J. Poellmann, K. L. Barton, S. Mishra, A. J. W. Johnson, *Macromol. Biosci.* **2011**, *11*, 1164.

[121] S. A. DeLong, J. J. Moon, J. L. West, *Biomaterials* **2005**, *26*, 3227.

[122] S. A. DeLong, A. S. Gobin, J. L. West, *J. Controlled Release* **2005**, *109*, 139.

[123] J. A. Burdick, A. Khademhosseini, R. Langer, *Langmuir* **2004**, *20*, 5153.

[124] Z. Liu, L. Xiao, B. Xu, Y. Zhang, A. F. T. Mak, Y. Li, W. Y. Man, M. Yang, *Biomicrofluidics* **2012**, *6*, 024111.

[125] M. V. Turturro, G. Papavasiliou, *J. Biomater. Sci., Polym. Ed.* **2012**, *23*, 917.

[126] S. Cosson, S. Allazetta, M. P. Lutolf, *Lab Chip* **2013**, *13*, 2099.

[127] S. G. M. Uzel, O. C. Amadi, T. M. Pearl, R. T. Lee, P. T. C. So, R. D. Kamm, *Small* **2016**, *12*, 612.

[128] D. Yoon, H. Kim, E. Lee, M. H. Park, S. Chung, H. Jeon, C. H. Ahn, K. Lee, *Biomater. Res.* **2016**, *20*, 25.

[129] O. Moreno-Arotzena, C. Borau, N. Movilla, M. Vicente-Manzanares, J. M. García-Aznar, *Ann. Biomed. Eng.* **2015**, *43*, 3025.

[130] N. Movilla, C. Borau, C. Valero, J. M. García-Aznar, *Bone* **2018**, *107*, 10.

[131] T. B. Tran, S. B. Cho, J. Min, *Biosens. Bioelectron.* **2013**, *50*, 453.

[132] S. García, R. Sunyer, A. Olivares, J. Noailly, J. Atencia, X. Trepat, *Lab Chip* **2015**, *15*, 2606.

[133] T. Kamperman, M. Koerselman, C. Kelder, J. Hendriks, J. F. Crispim, X. de Peuter, P. J. Dijkstra, M. Karperien, J. Leijten, *Nat. Commun.* **2019**, *10*, 4347.

[134] K. T. Dicker, A. C. Moore, N. T. Garabedian, H. Zhang, S. L. Scinto, R. E. Akins, D. L. Burris, J. M. Fox, X. Jia, *ACS Appl. Mater. Interfaces* **2019**, *11*, 16402.

[135] K. T. Dicker, J. Song, A. C. Moore, H. Zhang, Y. Li, D. L. Burris, X. Jia, J. M. Fox, *Chem. Sci.* **2018**, *9*, 5394.

[136] K. Abe, I. Kawamata, S. I. M. Nomura, S. Murata, *Mol. Syst. Des. Eng.* **2019**, *4*, 639.

[137] J. P. K. Armstrong, J. L. Puetzer, A. Serio, A. G. Guex, M. Kapnisi, A. Breant, Y. Zong, V. Assal, S. C. Skaalure, O. King, T. Murty, C. Meinert, A. C. Franklin, P. G. Bassindale, M. K. Nichols, C. M. Terracciano, D. W. Hutmacher, B. W. Drinkwater, T. J. Klein, A. W. Perriman, M. M. Stevens, *Adv. Mater.* **2018**, *30*, 1802649.

[138] Z. Ma, A. W. Holle, K. Melde, T. Qiu, K. Poeppel, V. M. Kadiri, P. Fischer, *Adv. Mater.* **2020**, *32*, 1904181.

[139] L. M. Johnson, C. A. DeForest, A. Pendurti, K. S. Anseth, C. N. Bowman, *ACS Appl. Mater. Interfaces* **2010**, *2*, 1963.

[140] C. C. Dufort, M. J. Paszek, V. M. Weaver, *Nat. Rev. Mol. Cell Biol.* **2011**, *12*, 308.

[141] R. J. Pelham, Y. L. Wang, *Proc. Natl. Acad. Sci. USA* **1997**, *94*, 13661.

[142] M. Dembo, Y. L. Wang, *Biophys. J.* **1999**, *76*, 2307.

[143] C. M. Lo, H. B. Wang, M. Dembo, Y. L. Wang, *Biophys. J.* **2000**, *79*, 144.

[144] C. R. Lee, A. J. Grodzinsky, M. Spector, *Biomaterials* **2001**, *22*, 3145.

[145] A. Banerjee, M. Arha, S. Choudhary, R. S. Ashton, S. R. Bhatia, D. V. Schaffer, R. S. Kane, *Biomaterials* **2009**, *30*, 4695.

[146] A. J. Engler, S. Sen, H. L. Sweeney, D. E. Discher, *Cell* **2006**, *126*, 677.

[147] O. Chaudhuri, L. Gu, M. Darnell, D. Klumpers, S. A. Bencherif, J. C. Weaver, N. Huebsch, D. J. Mooney, *Nat. Commun.* **2015**, *6*, 6365.

[148] S. Nam, R. Stowers, J. Lou, Y. Xia, O. Chaudhuri, *Biomaterials* **2019**, *200*, 15.

[149] O. Chaudhuri, L. Gu, D. Klumpers, M. Darnell, S. A. Bencherif, J. C. Weaver, N. Huebsch, H. P. Lee, E. Lippens, G. N. Duda, D. J. Mooney, *Nat. Mater.* **2016**, *15*, 326.

[150] A. P. Liu, O. Chaudhuri, S. H. Parekh, *Integr. Biol.* **2017**, *9*, 383.

[151] S. Dupont, L. Morsut, M. Aragona, E. Enzo, S. Giulitti, M. Cordenonsi, F. Zanconato, J. Le Digabel, M. Forcato, S. Bicciato, N. Elvassore, S. Piccolo, *Nature* **2011**, *474*, 179.

[152] B. D. Matthews, C. K. Thodeti, J. D. Tytell, A. Mammoto, D. R. Overby, D. E. Ingber, *Integr. Biol.* **2010**, *2*, 435.

[153] A. J. Maniotis, C. S. Chen, D. E. Ingber, *Proc. Natl. Acad. Sci. USA* **1997**, *94*, 849.

[154] C. M. Lo, H. B. Wang, M. Dembo, Y. L. Wang, *Biophys. J.* **2000**, *79*, 144.

[155] C. D. Hartman, B. C. Isenberg, S. G. Chua, J. Y. Wong, *Proc. Natl. Acad. Sci. USA* **2016**, *113*, 11190.

[156] D. Lee, K. Golden, M. M. Rahman, A. Moran, B. Gonzalez, S. Ryu, *Exp. Mech.* **2019**, *59*, 1249.

[157] W. J. Hadden, J. L. Young, A. W. Holle, M. L. McFetridge, D. Y. Kim, P. Wijesinghe, H. Taylor-Weiner, J. H. Wen, A. R. Lee, K. Bieback, B. N. Vo, D. D. Sampson, B. F. Kennedy, J. P. Spatz, A. J. Engler, Y. S. Cho, *Proc. Natl. Acad. Sci. USA* **2017**, *114*, 5647.

[158] S. Nemir, H. N. Hayenga, J. L. West, *Biotechnol. Bioeng.* **2010**, *105*, 636.

[159] K. Chatterjee, S. Lin-Gibson, W. E. Wallace, S. H. Parekh, Y. J. Lee, M. T. Cicerone, M. F. Young, C. G. Simon, *Biomaterials* **2010**, *31*, 5051.

[160] J. A. Burdick, A. Khademhosseini, R. Langer, *Langmuir* **2004**, *20*, 5153.

[161] G. Orsi, M. Fagnano, C. De Maria, F. Montemurro, G. Vozzi, *J. Tissue Eng. Regener. Med.* **2017**, *11*, 256.

[162] L. G. Vincent, Y. S. Choi, B. Alonso-Latorre, J. C. Del Álamo, A. J. Engler, *Biotechnol. J.* **2013**, *8*, 472.

[163] N. Zaari, P. Rajagopalan, S. K. Kim, A. J. Engler, J. Y. Wong, *Adv. Mater.* **2004**, *16*, 2133.

[164] B. C. Isenberg, P. A. DiMilla, M. Walker, S. Kim, J. Y. Wong, *Biophys. J.* **2009**, *97*, 1313.

[165] Y. K. Cheung, E. U. Azeloglu, D. A. Shiovitz, K. D. Costa, D. Seliktar, S. K. Sia, *Angew. Chem., Int. Ed.* **2009**, *48*, 7188.

[166] J. Y. Wong, A. Velasco, P. Rajagopalan, Q. Pham, *Langmuir* **2003**, *19*, 1908.

[167] R. Sunyer, A. J. Jin, R. Nossal, D. L. Sackett, *PLoS One* **2012**, *7*, 46107.

[168] C. L. Happe, K. P. Tenerelli, A. K. Gromova, F. Kolb, A. J. Engler, *Mol. Biol. Cell* **2017**, *28*, 1950.

[169] S. Kidoaki, T. Matsuda, *J. Biotechnol.* **2008**, *133*, 225.

[170] T. Kawano, S. Kidoaki, *Biomaterials* **2011**, *32*, 2725.

[171] S. Kidoaki, H. Sakashita, *PLoS One* **2013**, *8*, 78067.

[172] K. Moriyama, S. Kidoaki, *Langmuir* **2019**, *35*, 7478.

[173] H. Ebata, K. Moriyama, T. Kuboki, S. Kidoaki, *Biomaterials* **2020**, *230*, 119647.

[174] M. S. Hahn, J. S. Miller, J. L. West, *Adv. Mater.* **2006**, *18*, 2679.

[175] R. A. Marklein, J. A. Burdick, *Soft Matter* **2009**, *6*, 136.

[176] S. Khetan, J. A. Burdick, *Biomaterials* **2010**, *31*, 8228.

[177] M. Guvendiren, M. Perepelyuk, R. G. Wells, J. A. Burdick, *J. Mech. Behav. Biomed. Mater.* **2014**, *38*, 198.

[178] S. Khetan, J. A. Burdick, *Soft Matter* **2011**, *7*, 830.

[179] C. L. Petrou, T. J. D'Ovidio, D. A. Bölükbas, S. Tas, R. D. Brown, A. Allawzi, S. Lindstedt, E. Nozik-Grayck, K. R. Stenmark, D. E. Wagner, C. M. Magin, *J. Mater. Chem. B* **2020**, *8*, 6814.

[180] E. Hui, K. I. Gimeno, G. Guan, S. R. Caliari, *Biomacromolecules* **2019**, *20*, 4126.

[181] X. Tong, J. Jiang, D. Zhu, F. Yang, *ACS Biomater. Sci. Eng.* **2016**, *2*, 845.

[182] P. E. Farahani, S. M. Adelmund, J. A. Shadish, C. A. DeForest, *J. Mater. Chem. B* **2017**, *5*, 4435.

[183] K. A. Günay, T. L. Ceccato, J. S. Silver, K. L. Bannister, O. J. Bednarski, L. A. Leinwand, K. S. Anseth, *Angew. Chem., Int. Ed.* **2019**, *58*, 9912.

[184] M. T. Frey, Y. L. Wang, *Soft Matter* **2009**, *5*, 1918.

[185] A. M. Kloxin, M. W. Tibbitt, K. S. Anseth, *Nat. Protoc.* **2010**, *5*, 1867.

[186] A. M. Kloxin, J. A. Benton, K. S. Anseth, *Biomaterials* **2010**, *31*, 1.

[187] A. M. Kloxin, M. W. Tibbitt, A. M. Kasko, J. A. Fairbairn, K. S. Anseth, *Adv. Mater.* **2010**, *22*, 61.

[188] C. Xue, D. Y. Wong, A. M. Kasko, *Adv. Mater.* **2014**, *26*, 1577.

[189] F. Yanagawa, T. Mizutani, S. Sugiura, T. Takagi, K. Sumaru, T. Kanamori, *Colloids Surf., B* **2015**, *126*, 575.

[190] S. C. P. Norris, S. M. Delgado, A. M. Kasko, *Polym. Chem.* **2019**, *10*, 3180.

[191] H. Ma, A. R. Killaars, F. W. DelRio, C. Yang, K. S. Anseth, *Biomaterials* **2017**, *131*, 131.

[192] C. Yang, F. W. DelRio, H. Ma, A. R. Killaars, L. P. Basta, K. A. Kyburz, K. S. Anseth, *Proc. Natl. Acad. Sci. USA* **2016**, *113*, E4439.

[193] D. Xiang, X. Wu, W. Cao, B. Xue, M. Qin, Y. Cao, W. Wang, *Front. Chem.* **2020**, *8*, 7.

[194] L. Liu, J. A. Shadish, C. K. Arakawa, K. Shi, J. Davis, C. A. DeForest, *Adv. Biosyst.* **2018**, *2*, 1800240.

[195] M. Hörner, K. Raute, B. Hummel, J. Madl, G. Creusen, O. S. Thomas, E. H. Christen, N. Hotz, R. J. Gübeli, R. Engesser, B. Rebmann, J. Lauer, B. Rolauffs, J. Timmer, W. W. A. Schamel, J. Pruszak, W. Römer, M. D. Zurbriggen, C. Friedrich, A. Walther, S. Minguet, R. Sawarkar, W. Weber, *Adv. Mater.* **2019**, *31*, 1806727.

[196] S. M. Mehta, T. Jin, I. Stanciulescu, K. J. Grande-Allen, *Acta Biomater.* **2018**, *75*, 52.

[197] K. A. Mosiewicz, L. Kolb, A. J. Van Der Vlies, M. P. Lutolf, *Biomater. Sci.* **2014**, *2*, 1640.

[198] Z. Liu, Q. Lin, Y. Sun, T. Liu, C. Bao, F. Li, L. Zhu, *Adv. Mater.* **2014**, *26*, 3912.

[199] I. Mironi-Harpaz, L. Hazanov, G. Engel, D. Yelin, D. Seliktar, *Adv. Mater.* **2015**, *27*, 1933.

[200] K. C. Hribar, Y. S. Choi, M. Ondeck, A. J. Engler, S. Chen, *Adv. Funct. Mater.* **2014**, *24*, 4922.

[201] R. S. Stowers, S. C. Allen, L. J. Suggs, K. S. Anseth, *Proc. Natl. Acad. Sci. USA* **2015**, *112*, 1953.

[202] Y. Chandorkar, A. Castro Nava, S. Schweizerhof, M. Van Dongen, T. Haraszti, J. Köhler, H. Zhang, R. Windoffer, A. Mourran, M. Möller, L. De Laporte, *Nat. Commun.* **2019**, *10*, 4027.

[203] M. W. Tibbitt, A. M. Kloxin, K. U. Dyamenahalli, K. S. Anseth, *Soft Matter* **2010**, *6*, 5100.

[204] S. C. P. Norris, P. Tseng, A. M. Kasko, *ACS Biomater. Sci. Eng.* **2016**, *2*, 1309.

[205] M. A. Azagarsamy, D. D. McKinnon, D. L. Alge, K. S. Anseth, *ACS Macro Lett.* **2014**, *3*, 515.

[206] Y. S. Choi, L. G. Vincent, A. R. Lee, K. C. Kretchmer, S. Chirasatitsin, M. K. Dobke, A. J. Engler, *Biomaterials* **2012**, *33*, 6943.

[207] H. Zhang, F. Lin, J. Huang, C. Xiong, *Acta Biomater.* **2020**, *106*, 181.

[208] M. Diez, V. A. Schulte, F. Stefanoni, C. F. Natale, F. Mollica, C. M. Cesa, J. Chen, M. Möller, P. A. Netti, M. Ventre, M. C. Lensen, *Adv. Eng. Mater.* **2011**, *13*, B395.

[209] G. De Vicente, M. C. Lensen, *Eur. Polym. J.* **2016**, *78*, 290.

[210] C. H. R. Kuo, J. Xian, J. D. Brenton, K. Franze, E. Sivaniah, *Adv. Mater.* **2012**, *24*, 6059.

[211] P. hsiu, G. Chao, S. C. Sheng, W. R. Chang, *J. Mech. Behav. Biomed. Mater.* **2014**, *38*, 232.

[212] C. Kayal, E. Moeendarbary, R. J. Shipley, J. B. Phillips, *Adv. Healthcare Mater.* **2020**, *9*, 1901036.

[213] R. Yang, H. Liang, *RSC Adv.* **2018**, *8*, 6675.

[214] S. Riedel, K. Bela, E. I. Wisotzki, C. Suckfüll, J. Zajadacz, S. G. Mayr, *Mater. Des.* **2018**, *153*, 80.

[215] S. Riedel, B. Heyart, K. S. Apel, S. G. Mayr, *Sci. Rep.* **2017**, *7*, 17436.

[216] H. Yin, Y. Ding, Y. Zhai, W. Tan, X. Yin, *Nat. Commun.* **2018**, *9*, 1.

[217] K. Zhang, X. Xiao, X. Wang, Y. Fan, X. Li, *J. Mater. Chem. B* **2019**, *7*, 7090.

[218] A. Curtis, C. Wilkinson, *Biomaterials* **1997**, *18*, 1573.

[219] G. A. Dunn, T. Ebendal, *Exp. Cell Res.* **1978**, *111*, 475.

[220] D. M. Brunette, *Exp. Cell Res.* **1986**, *164*, 11.

[221] P. Clark, P. Connolly, A. S. G. Curtis, J. A. T. Dow, C. D. W. Wilkinson, *Development* **1990**, *108*, 635.

[222] C. S. Chen, M. Mrksich, S. Huang, G. M. Whitesides, D. E. Ingber, *Science* **1997**, *276*, 1425.

[223] S. Huang, C. S. Chen, D. E. Ingber, *Mol. Biol. Cell* **1998**, *9*, 3179.

[224] C. H. Seo, H. Jeong, Y. Feng, K. Montagne, T. Ushida, Y. Suzuki, K. S. Furukawa, *Biomaterials* **2014**, *35*, 2245.

[225] B. R. Hughes, M. Mirbagheri, S. D. Waldman, D. K. Hwang, *Acta Biomater.* **2018**, *78*, 89.

[226] S. Ostrovidov, V. Hosseini, S. Ahadian, T. Fujie, S. P. Parthiban, M. Ramalingam, H. Bae, H. Kaji, A. Khademhosseini, *Tissue Eng., Part B* **2014**, *20*, 403.

[227] J. Park, J. H. Choi, S. Kim, I. Jang, S. Jeong, J. Y. Lee, *Acta Biomater.* **2019**, *97*, 141.

[228] A. de Mel, G. Jell, M. M. Stevens, A. M. Seifalian, *Biomacromolecules* **2008**, *9*, 2969.

[229] C. Simitzi, A. Ranella, E. Stratakis, *Acta Biomater.* **2017**, *51*, 21.

[230] R. B. Vernon, M. D. Gooden, S. L. Lara, T. N. Wight, *Biomaterials* **2005**, *26*, 3131.

[231] E. Figallo, M. Flaibani, B. Zavan, G. Abatangelo, N. Elvassore, *Biotechnol. Prog.* **2007**, *23*, 210.

[232] M. C. Lensen, P. Mela, A. Mourran, J. Groll, J. Heuts, H. Rong, M. Möller, *Langmuir* **2007**, *23*, 7841.

[233] V. A. Schulte, M. Díez, M. Möller, M. C. Lensen, *Biomacromolecules* **2009**, *10*, 2795.

[234] H. G. Jayasinghe, C. J. Tormos, M. Khan, S. Madihally, Y. Vasquez, *J. Polym. Sci., Part B: Polym. Phys.* **2018**, *56*, 1144.

[235] P. Lavrador, V. M. Gaspar, J. F. Mano, *Adv. Healthcare Mater.* **2020**, *9*, 1901860.

[236] Y. Wang, R. Kim, D. B. Gunasekara, M. I. Reed, M. DiSalvo, D. L. Nguyen, S. J. Bultman, C. E. Sims, S. T. Magness, N. L. Allbritton, *Cell. Mol. Gastroenterol. Hepatol.* **2018**, *5*, 113.

[237] M. L. McCain, A. Agarwal, H. W. Nesmith, A. P. Nesmith, K. K. Parker, *Biomaterials* **2014**, *35*, 5462.

[238] A. Bettadapur, G. C. Suh, N. A. Geisse, E. R. Wang, C. Hua, H. A. Huber, A. A. Viscio, J. Y. Kim, J. B. Strickland, M. L. McCain, *Sci. Rep.* **2016**, *6*, 28855.

[239] L. Y. Jiang, Y. Luo, *Soft Matter* **2013**, *9*, 1113.

[240] K. Y. Suh, J. Seong, A. Khademhosseini, P. E. Laibinis, R. Langer, *Biomaterials* **2004**, *25*, 557.

[241] P. Kim, D. H. Kim, B. Kim, S. K. Choi, S. H. Lee, A. Khademhosseini, R. Langer, K. Y. Suh, *Nanotechnology* **2005**, *16*, 2420.

[242] D. H. Kim, P. Kim, I. Song, J. M. Cha, S. H. Lee, B. Kim, K. Y. Suh, *Langmuir* **2006**, *22*, 5419.

[243] P. Kim, A. Yuan, K. H. Nam, A. Jiao, D. H. Kim, *Biofabrication* **2014**, *6*, 024112.

[244] D. H. Kim, E. A. Lipke, P. Kim, R. Cheong, S. Thompson, M. Delannoy, K. Y. Suh, L. Tung, A. Levchenko, *Proc. Natl. Acad. Sci. USA* **2010**, *107*, 565.

[245] A. Agarwal, Y. Farouz, A. P. Nesmith, L. F. Deravi, M. L. McCain, K. K. Parker, *Adv. Funct. Mater.* **2013**, *23*, 3738.

[246] C. L. Nemeth, K. Janebodin, A. E. Yuan, J. E. Dennis, M. Reyes, D. H. Kim, *Tissue Eng., Part A* **2014**, *20*, 2817.

[247] J. Comelles, V. Fernández-Majada, N. Berlanga-Navarro, V. Acevedo, K. Paszkowska, E. Martínez, *Biofabrication* **2020**, *12*, 025023.

[248] V. A. Liu, S. N. Bhatia, *Biomed. Microdevices* **2002**, *4*, 257.

[249] S. J. Bryant, K. D. Hauch, B. D. Ratner, *Macromolecules* **2006**, *39*, 4395.

[250] S. J. Bryant, J. L. Cuy, K. D. Hauch, B. D. Ratner, *Biomaterials* **2007**, *28*, 2978.

[251] B. D. Fairbanks, S. P. Singh, C. N. Bowman, K. S. Anseth, *Macromolecules* **2011**, *44*, 2444.

[252] C. Xue, D. Y. Wong, A. M. Kasko, *Adv. Mater.* **2014**, *26*, 1577.

[253] C. M. Kirschner, K. S. Anseth, *Small* **2013**, *9*, 578.

[254] M. Nikkhah, N. Eshak, P. Zorlutuna, N. Annabi, M. Castello, K. Kim, A. Dolatshahi-Pirouz, F. Edalat, H. Bae, Y. Yang, A. Khademhosseini, *Biomaterials* **2012**, *33*, 9009.

[255] Y. Berkovitch, D. Yelin, D. Seliktar, *Eur. Polym. J.* **2015**, *72*, 473.

[256] X. H. Qin, J. Torgersen, R. Saf, S. Mühleder, N. Pucher, S. C. Ligon, W. Holnthoner, H. Redl, A. Ovsianikov, J. Stampfl, R. Liska, *J. Polym. Sci., Part A Polym. Chem.* **2013**, *51*, 4799.

[257] K. C. Hribar, K. Meggs, J. Liu, W. Zhu, X. Qu, S. Chen, *Sci. Rep.* **2015**, *5*, 17203.

[258] S. K. Seidlits, C. E. Schmidt, J. B. Shear, *Adv. Funct. Mater.* **2009**, *19*, 3543.

[259] M. Hippler, E. Blasco, J. Qu, M. Tanaka, C. Barner-Kowollik, M. Wegener, M. Bastmeyer, *Nat. Commun.* **2019**, *10*, 232.

[260] A. M. Kloxin, K. J. R. Lewis, C. A. DeForest, G. Seedorf, M. W. Tibbitt, V. Balasubramaniam, K. S. Anseth, *Integr. Biol.* **2012**, *4*, 1540.

[261] D. D. McKinnon, T. E. Brown, K. A. Kyburz, E. Kiyotake, K. S. Anseth, *Biomacromolecules* **2014**, *15*, 2808.

[262] C. K. Arakawa, B. A. Badeau, Y. Zheng, C. A. DeForest, *Adv. Mater.* **2017**, *29*, 1703156.

[263] D. Y. Wong, D. R. Griffin, J. Reed, A. M. Kasko, *Macromolecules* **2010**, *43*, 2824.

[264] N. Brandenberg, M. P. Lutolf, *Adv. Mater.* **2016**, *28*, 7450.

[265] C. Arakawa, C. Gunnarsson, C. Howard, M. Bernabeu, K. Phong, E. Yang, C. A. DeForest, J. D. Smith, Y. Zheng, *Sci. Adv.* **2020**, *6*, eaay7243.

[266] D. Li, Y. Xia, *Adv. Mater.* **2004**, *16*, 1151.

[267] M. V. Kakade, S. Givens, K. Gardner, K. H. Lee, D. B. Chase, J. F. Rabolt, *J. Am. Chem. Soc.* **2007**, *129*, 2777.

[268] Y. Liu, L. Zhang, H. Li, S. Yan, J. Yu, J. Weng, X. Li, *Langmuir* **2012**, *28*, 17134.

[269] K. Hou, H. Wang, Y. Lin, S. Chen, S. Yang, Y. Cheng, B. S. Hsiao, M. Zhu, *Macromol. Rapid Commun.* **2016**, *37*, 1795.

[270] L. Nivison-Smith, A. S. Weiss, *J. Biomed. Mater. Res., Part A* **2012**, *100A*, 155.

[271] T. Fee, S. Surianarayanan, C. Downs, Y. Zhou, J. Berry, *PLoS One* **2016**, *11*, 0154806.

[272] S. Yao, X. Liu, S. Yu, X. Wang, S. Zhang, Q. Wu, X. Sun, H. Mao, *Nanoscale* **2016**, *8*, 10252.

[273] T. Hu, Q. Li, H. Dong, W. Xiao, L. Li, X. Cao, *Small* **2017**, *13*, 1602610.

[274] S. H. Cha, H. J. Lee, W. G. Koh, *Biomater. Res.* **2017**, *21*, 1.

[275] W. Song, D. An, D. I. Kao, Y. C. Lu, G. Dai, S. Chen, M. Ma, *ACS Appl. Mater. Interfaces* **2014**, *6*, 7038.

[276] R. L. Truby, J. A. Lewis, *Nature* **2016**, *540*, 371.

[277] D. M. Kirchmajer, R. Gorkin, M. In Het Panhuis, *J. Mater. Chem. B* **2015**, *3*, 4105.

[278] K. Itoga, M. Yamato, J. Kobayashi, A. Kikuchi, T. Okano, *Biomaterials* **2004**, *25*, 2047.

[279] T. M. Valentin, S. E. Leggett, P. Y. Chen, J. K. Sodhi, L. H. Stephens, H. D. McClintock, J. Y. Sim, I. Y. Wong, *Lab Chip* **2017**, *17*, 3474.

[280] Y. Lu, G. Mapili, G. Suhali, S. Chen, K. Roy, *J. Biomed. Mater. Res., Part A* **2006**, *77A*, 396.

[281] P. Jiang, C. Yan, Z. Ji, Y. Guo, X. Zhang, X. Jia, X. Wang, F. Zhou, *ACS Appl. Mater. Interfaces* **2019**, *11*, 42586.

[282] D. Xue, J. Zhang, Y. Wang, D. Mei, *ACS Biomater. Sci. Eng.* **2019**, *5*, 4825.

[283] P. Soman, P. H. Chung, A. P. Zhang, S. Chen, *Biotechnol. Bioeng.* **2013**, *110*, 3038.

[284] R. Gauvin, Y. C. Chen, J. W. Lee, P. Soman, P. Zorlutuna, J. W. Nichol, H. Bae, S. Chen, A. Khademhosseini, *Biomaterials* **2012**, *33*, 3824.

[285] X. Ma, X. Qu, W. Zhu, Y. S. Li, S. Yuan, H. Zhang, J. Liu, P. Wang, C. S. E. Lai, F. Zanella, G. S. Feng, F. Sheikh, S. Chien, S. Chen, *Proc. Natl. Acad. Sci. USA* **2016**, *113*, 2206.

[286] F. Klein, B. Richter, T. Striebel, C. M. Franz, G. Von Freymann, M. Wegener, M. Bastmeyer, *Adv. Mater.* **2011**, *23*, 1341.

[287] J. A. Lewis, *Adv. Funct. Mater.* **2006**, *16*, 2193.

[288] R. A. Barry, R. F. Shepherd, J. N. Hanson, R. G. Nuzzo, P. Wiltzius, J. A. Lewis, *Adv. Mater.* **2009**, *21*, 2407.

[289] M. Müller, J. Becher, M. Schnabelrauch, M. Zenobi-Wong, *Biofabrication* **2015**, *7*, 035006.

[290] P. T. Smith, A. Basu, A. Saha, A. Nelson, *Polymer* **2018**, *152*, 42.

[291] W. Wu, A. Deconinck, J. A. Lewis, *Adv. Mater.* **2011**, *23*, H178.

[292] M. Zhang, A. Vora, W. Han, R. J. Wojtecki, H. Maune, A. B. A. Le, L. E. Thompson, G. M. McClelland, F. Ribet, A. C. Engler, A. Nelson, *Macromolecules* **2015**, *48*, 6482.

ADVANCED
Science News

www.advancedsciencenews.com

ADVANCED
MATERIALS
INTERFACES

www.advmatinterfaces.de

[293] A. Sheikhi, J. de Rutte, R. Haghniaz, O. Akouissi, A. Sohrabi, D. Di Carlo, A. Khademhosseini, *Biomaterials* **2019**, *192*, 560.

[294] J. M. de Rutte, J. Koh, D. Di Carlo, *Adv. Funct. Mater.* **2019**, *29*, 1900071.

[295] I. Saaem, J. Tian, *Adv. Mater.* **2007**, *19*, 4268.

[296] G. Dos Reis, F. Fenili, A. Gianfelice, G. Bongiorno, D. Marchesi, P. E. Scopelliti, A. Borgonovo, A. Podestà, M. Indrieri, E. Ranucci, P. Ferruti, C. Lenardi, P. Milani, *Macromol. Biosci.* **2010**, *10*, 842.

[297] S. Y. Chou, P. R. Krauss, P. J. Renstrom, *Appl. Phys. Lett.* **1995**, *67*, 3114.

[298] M. F. A. Cutiongco, S. H. Goh, R. Aid-Launais, C. Le Visage, H. Y. Low, E. K. F. Yim, *Biomaterials* **2016**, *84*, 184.

[299] J. D. Kiang, J. H. Wen, J. C. Del Álamo, A. J. Engler, *J. Biomed. Mater. Res., Part A* **2013**, *101A*, 2313.

[300] T. Tanaka, S. T. Sun, Y. Hirokawa, S. Katayama, J. Kucera, Y. Hirose, T. Amiya, *Nature* **1987**, *325*, 796.

[301] V. Trujillo, J. Kim, R. C. Hayward, *Soft Matter* **2008**, *4*, 564.

[302] M. Guvendiren, S. Yang, J. A. Burdick, *Adv. Funct. Mater.* **2009**, *19*, 3038.

[303] Y. Zhou, C. M. Duque, C. D. Santangelo, R. C. Hayward, *Adv. Funct. Mater.* **2019**, *29*, 1905273.

[304] S. J. Jeon, R. C. Hayward, *Soft Matter* **2020**, *16*, 688.

[305] A. M. Rosales, K. M. Mabry, E. M. Nehls, K. S. Anseth, *Biomacromolecules* **2015**, *16*, 798.

[306] A. M. Rosales, C. B. Rodell, M. H. Chen, M. G. Morrow, K. S. Anseth, J. A. Burdick, *Bioconjugate Chem.* **2018**, *29*, 905.

[307] A. M. Rosales, S. L. Vega, F. W. DelRio, J. A. Burdick, K. S. Anseth, *Angew. Chem., Int. Ed.* **2017**, *56*, 12132.

[308] S. Lyu, J. Fang, T. Duan, L. Fu, J. Liu, H. Li, *Chem. Commun.* **2017**, *53*, 13375.

[309] X. Wu, W. Huang, W. H. Wu, B. Xue, D. Xiang, Y. Li, M. Qin, F. Sun, W. Wang, W. Bin Zhang, Y. Cao, *Nano Res.* **2018**, *11*, 5556.

[310] Z. Yang, Y. Yang, M. Wang, T. Wang, H. K. F. Fok, B. Jiang, W. Xiao, S. Kou, Y. Guo, Y. Yan, X. Deng, W. Bin Zhang, F. Sun, *Matter* **2020**, *2*, 233.

[311] J. Allen, *Nat. Methods* **2017**, *14*, 1114.

[312] F. Schmieder, S. D. Klapper, N. Koukourakis, V. Busskamp, J. W. Czarske, *Appl. Sci.* **2018**, *8*, 1180.

[313] C. Maibohm, O. F. Silvestre, J. Borme, M. Sinou, K. Heggarty, J. B. Nieder, *Sci. Rep.* **2020**, *10*, 8740.

[314] B. W. Pearre, C. Michas, J. M. Tsang, T. J. Gardner, T. M. Otchy, *Addit. Manuf.* **2019**, *30*, 100887.

Brizzia G. Munoz-Robles is currently pursuing her Ph.D. degree in the Department of Bioengineering at the University of Washington, where she began in 2019. Her research interests include using light to control cell function in biomaterials.

Irina Kopyeva is an NSF Graduate Research Fellow at the University of Washington in the Department of Bioengineering, where she began in 2019. Her interests include developing biomaterials to better understand mechanotransduction and how this plays a role in cellular development and disease progression.

Cole A. DeForest is the Dan Evans Career Development Assistant Professor in the Departments of Chemical Engineering and Bioengineering at the University of Washington, where he began in 2014. His research program focuses on the development and exploitation of user-programmable biomaterials for 4D cell culture and targeted drug delivery.